RESEARCH ARTICLE OPEN ACCESS

Olive Leaf Extracts With High, Medium, or Low Bioactive Compounds Content Differentially Modulate Alzheimer's Disease via Redox Biology

Jose M. Romero-Marquez[1] | María D. Navarro-Hortal[1] | Alfonso Varela-López[1] | Rubén Calderón-Iglesias[2,3] | Juan G. Puentes[4] | Francesca Giampieri[2,5,6,7] | Maurizio Battino[2,5,6,7] 🔗 | Cristina Sánchez-González[1] 🔗 | Jianbo Xiao[8] 🔗 | Roberto García-Ruiz[4] | Sebastián Sánchez[4] | Tamara Y. Forbes-Hernández[1] | José L. Quiles[1,2] 🔗

[1]Department of Physiology, Institute of Nutrition and Food Technology "José Mataix Verdú", Biomedical Research Centre, University of Granada, Armilla, Spain | [2]Research Group on Foods, Nutritional Biochemistry and Health, Universidad Europea del Atlántico, Santander, Spain | [3]Department of Health, Nutrition and Sport, Iberoamericana International University, Campeche, Mexico | [4]University Institute of Research in Olive Grove and Olive Oils, University of Jaén, Jaén, Spain | [5]Joint Laboratory on Food Science, Nutrition, and Intelligent Processing of Foods, Polytechnic University of Marche, Italy, Universidad Europea del Atlántico Spain and Jiangsu University, China, Polytechnic University of Marche, Ancona, Italy | [6]Dipartimento di Scienze Cliniche Specialistiche e Odontostomatologiche, Polytechnic University of Marche, Ancona, Italy | [7]International Research Center for Food Nutrition and Safety, Jiangsu University, Zhenjiang, China | [8]Department of Analytical Chemistry and Food Science, Faculty of Food Science and Technology, Jiangsu University, Ourense, Spain

Correspondence: Tamara Y. Forbes-Hernández (tforbes@ugr.es) | José L. Quiles (jlquiles@ugr.es)

ABSTRACT

Alzheimer's disease (AD) involves β-amyloid plaques and tau hyperphosphorylation, driven by oxidative stress and neuroinflammation. Cyclooxygenase-2 (COX-2) and acetylcholinesterase (AChE) activities exacerbate AD pathology. Olive leaf (OL) extracts, rich in bioactive compounds, offer potential therapeutic benefits. This study aimed to assess the anti-inflammatory, anticholinergic, and antioxidant effects of three OL extracts (low, mid, and high bioactive content) in vitro and their protective effects against AD-related proteinopathies in *Caenorhabditis elegans* models. OL extracts were characterized for phenolic composition, AChE and COX-2 inhibition, as well as antioxidant capacity. Their effects on intracellular and mitochondrial reactive oxygen species (ROS) were tested in *C. elegans* models expressing human Aβ and tau proteins. Gene expression analyses examined transcription factors (DAF-16, skinhead [SKN]-1) and their targets (superoxide dismutase [SOD]-2, SOD-3, GST-4, and heat shock protein [HSP]-16.2). High-OL extract demonstrated superior AChE and COX-2 inhibition and antioxidant capacity. Low- and high-OL extracts reduced Aβ aggregation, ROS levels, and proteotoxicity via SKN-1/NRF-2 and DAF-16/FOXO pathways, whereas mid-OL showed moderate effects through proteostasis modulation. In tau models, low- and high-OL extracts mitigated mitochondrial ROS levels via SOD-2 but had limited effects on intracellular ROS levels. High-OL extract also increased GST-4 levels, whereas low and mid extracts enhanced GST-4 levels. OL extracts protect against AD-related proteinopathies by modulating

Jose M. Romero-Marquez and María D. Navarro-Hortal contributed equally to this work.

- -

oxidative stress, inflammation, and proteostasis. High-OL extract showed the most promise for nutraceutical development due to its robust phenolic profile and activation of key antioxidant pathways. Further research is needed to confirm long-term efficacy.

1 | Introduction

The pathophysiology of Alzheimer disease (AD) is well known to involve two histopathological hallmarks: the aggregation of β-amyloid protein (Aβ) and the hyperphosphorylation of tau protein, which leads to the formation in the brain of Aβ-plaques and neurofibrillary tangles (NFTs), respectively (Guan et al. 2019). However, the reason for the deposition and aggregation remains unclear. Some authors demonstrated the role of oxidative stress and neuroinflammation in AD progression through the regulation of Aβ and tau hyperphosphorylation and deposition (Everett et al. 2018; Ho et al. 1999). Concerning neuroinflammation, it has been found that cyclooxygenase (COX)-2 expression was increased in the brain of AD patients (Ho et al. 1999, 2001; Pasinetti and Aisen 1998; Xiang et al. 2018). This COX-2 elevation has been epidemiologically correlated with the severity of AD pathology in humans (Ho et al. 1999, 2001). In the same way, animal studies revealed that COX-2 has an important role in spreading Aβ deposits as well as increasing the tau-pathology (Guan et al. 2019). In this context, numerous authors have shown that drugs that could selectively inhibit COX-2 might reduce the clinical aspects of AD (in t' Veld et al. 2001; McGeer et al. 1996; Stewart et al. 1997). Nonetheless, the posology of these drugs has been associated with numerous side effects (Steinman et al. 2006). In the same way, oxidative stress and redox-active iron accumulation have been detected as an early mark in AD pathophysiology, which has been described as a key factor in the formation of Aβ-plaque cores (Everett et al. 2018). During AD, reactive iron species can react with numerous biomolecules through hydroxyl radical generation, producing reactive oxygen species (ROS), which contribute to oxidative stress (Zhao 2019). Hydroxyl radicals can initiate lipid peroxidation in the brain, resulting in successive liberation of redox-active iron into the cytosol. This leads to increased concentration of labile iron pools that may cause cell damage and result in ferroptosis reported in this neurodegenerative process (Morris et al. 2018).

Beyond the amyloid and tau propagation theories, alternative explanations for the progression of AD have been proposed. Davies and Maloney (1976) introduced the cholinergic hypothesis of AD, which highlights alterations in acetylcholine (ACh) concentration in neurons during the AD pathogenesis. Specifically, it suggests hyperactivity of acetylcholinesterase (AChE), favoring the degradation of ACh and promoting that AD patients develop severe ACh deficiency in the brain. This brain ACh deficit has been associated with memory loss and other cognitive symptoms related to AD (Terry and Buccafusco 2003). Consequently, inhibiting AChE can extend cholinergic transmission and enhance signaling. AChE inhibitors remain the only approved pharmacological treatment for AD. Nowadays, the most widely used AChE inhibitors are physostigmine, donepezil, rivastigmine, and galantamine, which exhibit an amelioration of AD symptoms without preventing the brain damage. However, due to the significant side effects, the use of these AChE inhibitors is limited (Chen et al. 2022).

Bioactive compounds in foods, such as polyphenols, flavonoids, and antioxidants, play a crucial role in promoting health by reducing oxidative stress and inflammation. A balanced diet rich in these compounds supports overall well-being, aids in preventing chronic diseases, and enhances long-term health and vitality (Godos et al. 2024; Qi et al. 2024; Regolo et al. 2024; Rosi et al. 2024, 5; Saz-Lara et al. 2024). The use of natural by-products with antioxidant activity and nutraceutical potential might be an interesting approach for adjuvant therapy for AD. For this purpose, olive leaf (OL) extract might be an excellent candidate as a nutraceutical tool for AD therapy. OLs are rich in numerous compounds with biomedical properties, such as flavonoids, secoiridoids, phenolic alcohols, and phenolic acids that may be used for nutraceutical development (Romero-Márquez et al. 2023a; Romero-Márquez et al. 2022a). In particular, OLs have demonstrated important biomedical properties, such as antiviral, anti-microbial, anti-inflammatory, antioxidant, anti-aging, and anti-AD activities (Alcántara et al. 2020; Lama-Muñoz et al. 2020; Romero-Márquez et al. 2021; Romero-Márquez et al. 2023a). In the present research, an in-depth phytochemical characterization was conducted, focusing on the anti-cholinergic, anti-inflammatory, and anti-oxidative effects of three OL extracts varying in their phytochemical composition from a cohort of 50 samples from 5 countries. Similarly, the potential therapeutic effect against ad-related proteinopathies, including Aβ and tau protein–induced toxicity in vivo, was studied using *Caenorhabditis elegans*, aiming to elucidate the molecular basis of the observed protective effects.

2 | Materials and Methods

2.1 | Chemicals and Reagents

All reagents were of analytical grade and were purchased from Sigma-Aldrich (St. Louis, Missouri, USA), Thermo Fisher (Waltham, Massachusetts, USA), Extrasynthese (Genay Cedex, France), Agilent Technologies (Santa Clara, CA, USA), Roche (Basel, Switzerland), Panreac (Barcelona, Spain), or Merck (Darmstadt, Germany). Double-distilled deionized water was obtained from a Milli-Q purification system from Millipore (Milford, MA, USA).

2.2 | OL Obtention and Extraction

For the present study, three individuals from a cohort of 50 OL samples from 5 different countries, namely, Spain, Italy, Greece, Portugal, and Morocco, coming from previous research (Romero-Márquez et al. 2024) were investigated. The OLs utilized were gathered during the olive harvesting process, excluding

leaves from the ground or directly picked from trees. These samples underwent drying, grinding, and sieving to obtain a fine powder. The resulting OL powder was then blended with an extraction buffer (composed of ethanol, Milli-Q water, and formic acid in a ratio of 80:20:0.1, v:v:v) and mixed in darkness at room temperature for 2 h. Subsequently, the OL mixture underwent centrifugation, and the supernatant was filtered through a 0.45 μm syringe filter (PBI International, Italy). Finally, the samples were portioned, evaporated using a Speedvac SC110A (New York, USA), and stored at −80°C until further analysis.

2.3 | Identification and Quantification of the Phytochemical Compounds via High-Performance Liquid Chromatography (HPLC)-ESI-QTOF-MS/MS Analysis

HPLC analyses were performed on an Agilent 1260 HPLC instrument (California, USA) equipped with a binary pump, an online degasser, an auto-sampler, a thermo-statically controlled column compartment, and a diode array detector (Romero-Márquez et al. 2024). The samples were separated on an Agilent Zorbax Eclipse Plus C18 column (1.8 μm, 4.6 × 150 mm2). The mobile phases consisted of water with 0.1% formic acid (A) and methanol with 0.1% formic acid (B) using a gradient elution according to the following profile: 0 min, 5% B; 5 min, 75% B; 10 min, 100% B; 18 min, 100% B; 25 min, 5% B. The initial conditions were maintained for 5 min. The flow rate was 0.8 mL/min, the column temperature was 30°C, and the injection volume was 5 μL. The compound concentrations of each OL extract were determined using the area of each individual compound and by interpolation in the corresponding calibration curve. Oleuropein, hydroxytyrosol, luteolin, luteolin-7-O-glucoside, and verbascoside were quantified by the calibration curves obtained from their respective commercial standards. The remaining compounds were tentatively quantified on the basis of calibration curves from other compounds with structural similarities. Results are expressed as mean ± standard deviation (SD).

2.4 | Total Phenolic Content (TPC)

TPC and flavonoid content (TFC) of OL extracts were assessed by colorimetric procedures following the same protocol previously published by Romero-Márquez, Navarro-Hortal et al. (2023b) and Navarro-Hortal et al. (2022). Results were presented as milligrams (mg) of gallic acid (GA) equivalent per gram of dry weight (DW) extract for phenolics determination or mg of catechin equivalents (CAT)/g of DW extract for flavonoids measurement. Results are expressed as mean ± SD.

2.5 | AChE Inhibition Assay

The AChE inhibition assay of OL extracts was performed using the colorimetric method proposed by Ellman et al. (1961) with some modifications as previously described (Romero-Márquez et al. 2024). The concentration of the selected extracts causing 50% inhibition of the AChE activity (IC50) was calculated using linear regression analysis. Results are expressed as mean ± standard error of the mean (SEM).

2.6 | COX-2 Inhibition Assay

The COX-2 inhibition assay of OL was performed via Biovision COX-2 Inhibitor Screening Kit (California, USA) following the manufacturer's instructions as previously described (Romero-Márquez, Navarro-Hortal, et al. 2023b). The concentration of the selected extracts causing 50% inhibition of the COX-2 activity (IC50) was calculated using linear regression analysis. Results are expressed as mean ± SEM.

2.7 | Total Antioxidant Capacity (TAC)

TAC of the studied OL was determined by using three different methods based on electron transfer (ET). The ET-based methods analyze the ability of a specific antioxidant to reduce an oxidant, changing the color during this reaction. The magnitude of the color change is directly associated with the antioxidant concentration in the sample (D. Huang et al. 2005). In this context, 2,2′-azino-bis(3-ethylbenzothiazoline-6-sulfonic acid) (ABTS), ferric reducing antioxidant power (FRAP), and 2,2-diphenyl-1-picrylhydrazyl (DPPH) methods were performed following the modified protocols described by Navarro-Hortal et al. (2022) and Rivas-García et al. (2022). Results were expressed as μM of Trolox/g of DW extract for the three methods. Results are expressed as mean ± SD.

2.8 | Maintenance and Strains

All strains of *C. elegans* were obtained from the CGC (Minneapolis, MI, USA) and were housed at 20°C on solid nematode growth medium (NGM) plates fed with *Escherichia coli* OP50 in an incubator (VELP Scientifica FOC 120 E, Usmate, Italy). The strains used were as follows: N2-Wild type, LD1 *skn-1*::GFP (*ldIs7*); TJ356 *daf-16p*::GFP (*zIs356*); OS3062 *hsf-1*::GFP (*nsEx1730*); TJ375 *hsp-16.2p*::GFP (*gpIs1*); CF1553 *sod-3p*::GFP (*muIs84*); and CL2166 *gst-4p*::GFP (*dvIs19*), BR5706 (*bkIs10*), CL802 (*smg-1*), and CL4176 (*dvIs27*). Only CL4176 and CL802 were housed at 16°C. For experiments, a bleaching method was used to obtain age-matched embryos according to standard protocols (Porta-de-la-Riva et al. 2012). Briefly, worms were washed and collected with M9 buffers, and embryos were isolated using bleaching solution (sodium hypochlorite 4% and NaOH 0.5 N [20/80; v/v]). Then, embryos were washed three times and dispensed into experimental plates.

2.9 | Aβ-Induced Toxicity Test

Aβ-induced toxicity tolerance test was performed to determine the potential effect of OL extracts against amyloidogenic toxicity (Romero-Márquez et al. 2022b). For this purpose, CL4176 was used. CL4176 is a temperature-sensitive strain that expresses human amyloid β_{1-42} peptide in muscle cells, which causes a progressive impairment of movement until worms become paralyzed. CL802 was used as a negative control. Briefly, embryos from CL4176 Aβ (Aβ+) or CL802 Aβ (Aβ−) were placed in plates with 500 μg/mL of OL extracts or vehicle for 48 h at 16°C. Next, nematodes were temperature-up-shifted to 25°C for 22 h to induce endogenous Aβ production. Then, nematodes were counted every 2 for 12 h. Animals were classified as paralyzed if

they did not respond to physical stimuli in the lower two-thirds of their body but were still alive, as evidenced by head movement or pharyngeal pumping. Results are expressed as the percentage of non-paralyzed worms from 3 independent experiments with, at least, 100 worms per treatment and experiment.

2.10 | Thioflavin T Staining

Thioflavin T stain was used with the aim of visualizing Aβ aggregates in the CL4176 strain. Worms and plates were treated as paralysis assays. Synchronized CL4176 or CL802 eggs were placed on plates with the treatments and the control, seeded with *E. coli* OP50. After the incubation at 16°C for 48 h, all the plates were moved to another incubator at 25°C. Approximately at the time for 50% paralysis of the non-treated group, the nematodes were collected by washes with M9 buffer and fixed with 4% paraformaldehyde (pH 7.4) at 4°C for 24 h. After fixation, worms were permeabilized in 5% β-mercaptoethanol, 1% Triton X-100, and 125 mM Tris, pH 7.4, at 37°C for 24 h. Next, two washes with M9 buffer were performed to remove the permeabilization buffer. Then, samples were stained with 0.125% thioflavin T in 50% ethanol for 30 min and destained with sequential ethanol washes (50%, 75%, 90%, 75%, and 50% v/v), each one for 2 min (Navarro-Hortal et al. 2022). Thioflavin T–stained worms were observed under a Nikon epi-fluorescence microscope (Eclipse Ni, Nikon, Tokyo, Japan), and images were acquired at 40× magnification using the GFP filter with a Nikon DS-Ri2 camera (Tokyo, Japan). CL802-untreated worms were considered negative control, and the untreated CL4176 was the positive control, both incubated at 25°C.

2.11 | Hyperphosphorylated Tau-Induced Neurotoxicity Test

Tau protein–induced toxicity test was performed to evaluate the potential effect of OL extracts to front the neurotoxicity related to hyperphosphorylated tau protein (p-tau) aggregation (Romero-Márquez et al. 2022b). BR5706 strain was used for this experiment. These worms express a constitutive pro-aggregative human tau protein in neurons, reflecting in locomotion alterations. In this assay, embryos from BR5706 were placed in plates with 500 μg/mL of OL extracts or vehicle for 72 h at 20°C. Then, worms were moved to a slide with M9 to stimulate animal locomotion. Worm-Lab Imaging System (MBF Bioscience, Williston, Vermont, EE. UU) was used to document, track, and analyze worm movement. Activity and swimming speed were selected as demonstrative parameters to evaluate mobility alterations. Results are expressed as a percentage of fold change with respect to the positive control of the average of activity and swimming speed. Three independent experiments were conducted, each involving a minimum of 80 nematodes per treatment.

2.12 | Expression Level Analysis of Antioxidant and Proteostasis System

Different worm strains containing transgenic genes coupled to the GFP reporter were used to observe the mechanisms under the protective role of OL extracts in vivo (Navarro-Hortal et al. 2022). The transcription factors studied using different strains were skinhead [SKN]-1 (LD1), DAF-16 (TJ356), and heat shock transcription factor (HSF)-1 (OS3062). Among the downstream targets of the evaluated transcriptional factors, superoxide dismutase [SOD]-3 (CF1553), heat shock protein [HSP]-16.2 (TJ375), and GST-4 (CL2166) were analyzed. For this purpose, all strains were placed in plates with 500 μg/mL of OL extracts or vehicle for 48 h. Then, nematodes were moved to a slide and anesthetized with sodium azide (15 μM). A Nikon DS-Ri2 camera was used to photograph the worms under the GFP filter (Tokyo, Japan) in the region of interest (Table S1). Finally, to process the obtained images, the software NIS-Elements BR was used, and the background signal was removed from the analysis (Nikon, Tokyo, Japan). For gene expression analysis in each strain, results are presented as a fold change percentage of fluorescence intensity with respect to the control. Three independent experiments were conducted, each involving a minimum of 90 nematodes per treatment. An exception was made for TJ356 results, which are presented as the percentage of fold change with respect to the control of the average of a semi-quantitative scale (cytosolic "1," intermediate "2," or nuclear "3") of DAF-16::GFP location.

2.13 | Intracellular ROS Content

Intracellular ROS levels were measured in both C. elegans AD models. Therefore, the current study employed the 2′,7-dichlorodihydrofluorescein diacetate (H2DCFDA) staining method to assess intracellular ROS levels (Navarro-Hortal et al. 2024). The nematodes from CL802 and CL4176, as well as BR5706, were grown in the same conditions as those exposed for Aβ and p-tau toxicity tests, respectively. For the amyloidogenic strain, the measurement of intracellular ROS content was made at the 24-h mark after the temperature upshift, whereas in the tauopathy strain, the analysis was conducted at 74 h post-embryo bleaching. For both cases, the dye was applied in the same form: Nematodes were washed with M9 and exposed to 25 μM of H2DCFDA for 2 h. Finally, yellow fluorescence intensity as well as the time of flight (TOF) signal were measured using a BioSorter flow cytometer (Union Biometrica, Belgium, Europe). Results are expressed as a percentage of fold change with respect to the positive control of the mean of yellow intensity of fluorescence normalized by TOF signal. Three independent experiments were conducted, each involving a minimum of 1000 nematodes per treatment.

2.14 | Mitochondrial ROS Content

Mitochondrial ROS levels were measured in both C. elegans AD models. Therefore, the current study employed the MitoTracker Red CM-H2XRos staining method to assess mitochondrial ROS levels in the same conditions as intracellular ROS content (Navarro-Hortal et al. 2024). For dye application, the nematodes were washed with M9 and transferred to NGM plates containing 10 μM MitoTracker mixed with dead E. coli OP50 as a food source for 2 h. Finally, red fluorescence intensity as well as the TOF signal was measured using a BioSorter flow cytometer (Union Biometrica, Belgium, Europe). Results are expressed as a percentage of fold change with respect to the positive control of the mean of red intensity of fluorescence normalized by TOF

signal. Three independent experiments were conducted, each involving a minimum of 1000 nematodes per treatment.

2.15 | Glutathione (GSH) Content

Monochlorobimane (MCB) staining method was used to determinate the total GSH content in both *C. elegans* AD models (Navarro-Hortal et al. 2024). For the dye application, worms were washed with M9 buffer; subsequently, they were exposed to a permeabilization buffer (M9 buffer with 1% Triton X). Following this, the nematodes were divided into two groups: the stained group, treated with 200 μM MCB, and the unstained group, treated with an equivalent amount of DMSO as a control. After an incubation period of 1 h in the dark, at a temperature of 20°C, another wash step was performed using M9 buffer. Following the washing, the samples were read using a Synergy Neo2 microplate reader (Biotek, Winooski, Vermont, USA) operating in single reading mode. The measurements were taken at specific wavelengths: excitation at 380/20 nm and emission at 480/20 nm. Three independent experiments were conducted.

2.16 | RNAi Experiments

The inhibition of target gene expression was performed using the RNAi technique (Romero-Márquez et al. 2022b). This experiment was applied to the paralysis test and to the transgenic reporter strains. E. coli HT115 expressing DAF-16/FOXO (accession number: AF032112.1), SOD-2 (accession number: NM_059889.7), SOD-3 (accession number: NM_078363.9) (Cultek SL, Madrid, Spain), SKN-1/NRF2 (accession number: NM_171347.7), and HSP-16.2 (accession number: NM_001392482.1) (Sources BioScience, Nottingham, UK) was used to feed nematodes. RNAi plates were prepared by adding dsRNA to NGM containing 25 μg/mL carbenicillin and 1 mM isopropyl β-d-1-thiogalactopyranoside (IPTG). F0 (L3-L4 synchronized worms) growing in non-treated plates were moved to the RNAi dishes. When animals reached fertile age, the eggs (F1) were isolated through the bleaching method. For CL4176 and BR5706, used in the paralysis and movement test, respectively, those eggs were placed on plates containing treatments with each RNAi and a control plate without the RNAi. From this point, the experiments were carried out as described above.

2.17 | Statistical Analysis

The experimental procedures were performed at least three times. Statistical analysis was conducted using SPSS 24.0 software (IBM, Armonk, NY, USA) to assess normality, variance homogeneity, and perform analysis of variance (ANOVA). Post hoc Duncan's multiple range test was applied, with significance set at $p < 0.05$. Results are presented as the mean ± SD for OL extract characterization and as the mean ± SEM for *C. elegans* experiments.

3 | Results and Discussion

3.1 | OL Extract Selection, Phytochemical Profile, and Antioxidant Capacity In Vitro

To select the three extracts used in the present study, a categorization system was established and applied to a cohort of 50 OL samples previously characterized (Romero-Márquez et al. 2024). Here, the OL samples were classified into three categories, low, medium, and high, based on parameters such as inhibitory activity of AChE and COX-2 as well as FRAP, TPC, and TFC values. The low category contained 10% of the samples that obtained the lowest score. Similarly, the medium category contained 10% of the samples close to the population mean ($\bar{X}1$–50) for each parameter, whereas the high category contained 10% of the samples with the highest activities in the tests. The selection process involved ranking samples within each category based on the mentioned parameters. Scores were assigned, and an average was calculated for each sample, determining the sample selection score in each category. Three samples were chosen for further analysis based on their distinct biomedical and phytochemical properties (Figure S1): SU11 (lowest activity and content, low-OL), SU42 (medium activity and content, mid-OL), and SU04 (highest activity and content, high-OL).

After the OL extract selection process, the individual phytochemical characterization is presented in Table 1 and Table S2. As shown in Table 1, the low-OL extract contained only 7.1% of the secoiridoids studied, whereas the mid- and high-OL extracts contained 57.1% of the studied secoiridoids. Among the studied secoiridoids, the high-OL sample was the source of oleuropein and oleoside and its derivatives, as well as ligstroside, whereas the mid-OL extract had a secoiridoid content that was similar to the $\bar{X}1$–50.

Concerning flavonoid contents, the low-OL extract contained only 31.3% of the flavonoids studied, whereas the mid- and high-OL extracts contained 68.8% of the studied flavonoids. It should be highlighted the differences between mid- and high-OL extracts. Mid-OL extract was mostly a source of apigenin derivatives, whereas high OL-extract was mostly a source of luteolin derivatives. Among the other compounds with modulatory proved effects, the hydroxytyrosol, hydroxytyrosol glucoside, and verbascoside content were found to be higher than the $\bar{X}1$–50 in the high-OL extract. In contrast, these compounds were found to be lower than in the $\bar{X}1$–50 or even not detected in the mid- and low-OL extracts.

3.2 | In Vitro Inhibition of AChE and COX-2 by the Three-OL Extracts

The high-OL extract demonstrated the lowest IC_{50} for AChE inhibition, indicating a higher efficacy compared to the low-OL extract (Table 2). Isolated compounds, hydroxytyrosol and luteolin-7-*O*-glucoside, exhibited stronger AChE inhibitory activity, surpassing the high-OL extract by 26.6. Oleuropein displayed significant but lower AChE inhibitory activity, potentially contributing to the overall modulatory effect of the high-OL extract (Table 2).

TABLE 1 | Phytochemical compounds quantification of the three olive leaf (OL) extracts.

	$\bar{X}$1–50	Low-OL	Mid-OL	High-OL
Secoiridoids				
1-β-D-Glu-ACD EA I1	0.307 ± 0.203[b]	—	0.621 ± 0.021[c]	—
1-β-D-Glu-ACD EA I2	0.637 ± 0.560[b]	—	0.197 ± 0.002[a]	0.239 ± 0.007[a]
A-DM EA	0.180 ± 0.278[b]	—	0.374 ± 0.008[c]	—
Hy-DA-DM EA I1	0.104 ± 0.119[b]	—	0.153 ± 0.020[c]	—
Hy-DA-DM EA I2	0.198 ± 0.346[b]	0.051 ± 0.007[a]	—	—
Hydroxyoleuropein	0.235 ± 0.448[b]	—	0.220 ± 0.016[b]	0.937 ± 0.051[c]
Ligstroside	0.115 ± 0.292[b]	—	—	0.910 ± 0.027[c]
Oleoside	0.997 ± 1.85[b]	—	0.187 ± 0.003[a]	2.96 ± 0.088[c]
Oleoside methyl ester	0.772 ± 1.28[b]	—	0.597 ± 0.041[b]	4.35 ± 0.125[c]
Oleuropein	5.85 ± 14.0[b]	—	1.80 ± 0.021[a]	19.0 ± 0.891[c]
Oleuropein diglu	0.060 ± 0.173[b]	—	—	0.936 ± 0.081[c]
Oleuropein I	0.555 ± 1.44[b]	—	—	3.30 ± 0.082[c]
Flavonoids				
(+)-Eriodictyol	0.082 ± 0.109[b]	—	0.285 ± 0.007[c]	0.011 ± 0.002[a]
Apigenin	0.181 ± 0.223[b]	0.024 ± 0.004[a]	0.252 ± 0.001[b]	—
Apigenin-7-O-glu	0.279 ± 0.210[b]	—	0.431 ± 0.008[c]	0.566 ± 0.001[c]
Apigenin-7-O-rut	0.400 ± 0.222[b]	—	0.733 ± 0.006[c]	0.365 ± 0.014[b]
Azelaic acid	0.574 ± 0.775[b]	0.045 ± 0.001[a]	1.16 ± 0.011[c]	0.325 ± 0.003[b]
Chrysoeriol-7-O-glu	0.547 ± 0.251[b]	—	0.596 ± 0.011[b]	0.956 ± 0.009[c]
Diosmetin	0.226 ± 0.160[b]	0.104 ± 0.002[a]	0.257 ± 0.001[b]	—
I-3-O-β-D-glu	0.028 ± 0.050[b]	—	—	0.238 ± 0.012[c]
Luteolin	0.291 ± 0.203[b]	0.068 ± 0.001[a]	0.121 ± 0.002[a]	0.156 ± 0.008[a]
Luteolin 7-O-glu	1.09 ± 1.10[b]	—	0.657 ± 0.016[a]	4.33 ± 0.107[c]
Luteolin glu	3.81 ± 2.20[b]	0.163 ± 0.001[a]	6.99 ± 0.161[c]	6.72 ± 0.076[c]
Luteolin rut I2	0.018 ± 0.042[b]	—	—	0.039 ± 0.008[c]
Luteolin-7,4-O-diglu	0.084 ± 0.077[b]	—	0.143 ± 0.000[c]	0.171 ± 0.001[c]
Phenolic alcohols				
Hydroxytyrosol	0.131 ± 0.131[b]	—	0.056 ± 0.001[a]	0.471 ± 0.031[c]
Hydroxytyrosol glu	0.355 ± 0.515[b]	—	0.058 ± 0.001[a]	1.52 ± 0.007[c]
4-Ethylguaiacol	0.094 ± 0.071[b]	0.084 ± 0.005[a]	0.073 ± 0.000[a]	—
Iridoids				
Loganic acid	0.223 ± 0.101[b]	0.017 ± 0.000[a]	0.227 ± 0.005[b]	0.411 ± 0.003[c]
7-Epiloganin	0.667 ± 0.298[b]	0.122 ± 0.005[a]	0.944 ± 0.005[c]	0.995 ± 0.006[c]
Lamiol	0.778 ± 0.459[b]	0.089 ± 0.000[a]	1.12 ± 0.002[c]	0.819 ± 0.017[b]
Hydroxycoumarins				
Esculetin	0.179 ± 0.205[b]	0.012 ± 0.001[a]	0.148 ± 0.001[b]	0.115 ± 0.002[b]
Esculin	0.054 ± 0.049[b]	—	0.091 ± 0.001[c]	0.052 ± 0.001[b]
Hydroxycinnamic acid				
Verbascoside	0.307 ± 0.408[b]	0.043 ± 0.001[a]	0.083 ± 0.002[a]	0.545 ± 0.006[c]
Decaffeoylverbascoside	1.17 ± 0.842[b]	0.090 ± 0.004[a]	1.21 ± 0.049[b]	1.33 ± 0.018[b]

(Continues)

TABLE 1 | (Continued)

	X̄1–50	Low-OL	Mid-OL	High-OL
Phenolic acids				
p-Hydroxybenzoic acid	0.037 ± 0.059[b]	—	0.031 ± 0.001[b]	0.415 ± 0.001[c]
Other compounds				
Lauroside B	0.343 ± 0.329[b]	—	0.418 ± 0.003[b]	0.928 ± 0.025[c]

Note: Results are expressed as milligrams of compound (mean ± SD) per gram of dry weight. For each compound, different letters among extracts indicate statistically significant differences (p < 0.05). The symbol (—) was added when the specific compound was not detected.

Abbreviations: 1-*β*-D-Glu-ACD elenolic acid I1, 1-*β*-D-glucopyranosyl acyclodihydroelenolic acid isomer 1; 1-*β*-D-Glu-ACD elenolic acid I2, 1-*β*-D-glucopyranosyl acyclodihydroelenolic acid isomer 2; A-DM elenolic acid, aldehydic form of decarboxymethyl elenolic acid; D-OH elenolic acid I2, decarboxylated form of hydroxy elenolic acid isomer 2; glu, glucoside; H-DA-DM elenolic acid, hydrated product of the dialdehydic form of decarboxymethyl elenolic acid; Hy-DA-DM elenolic acid I1, hydroxylated product of the dialdehydic form of decarboxymethyl elenolic acid isomer 1; Hy-DA-DM elenolic acid I2, hydroxylated product of the dialdehydic form of decarboxymethyl elenolic acid isomer 2; I, isomer; OL, olive leaf; rut, rutinoside; X̄1–50, median from the cohort of 50 samples.

TABLE 2 | IC$_{50}$ for acetylcholinesterase (AChE) and cyclooxygenase-2 (COX-2) inhibitory activity assay for olive leaf extracts and some pure bioactive compounds from olive leaves.

	IC$_{50}$ (µg/mL)	R^2	Linear regression formula
AChE inhibitory activity			
Oleuropein	225	0.971	$y = 3.7771x + 36.555$
Hydroxytyrosol	50.6	0.986	$y = 1.1012x - 4.4927$
Luteolin-7-*O*-glu	50.7	0.949	$y = 0.6644x + 17.497$
Low-OL	6331	0.990	$y = 135.6x - 448.66$
Mid-OL	1444	0.994	$y = 43.311x - 721.92$
High-OL	1350	0.982	$y = 35.49x - 424.69$
COX-2 inhibitory activity			
Oleuropein	8.38	0.938	$y = 0.1843x + 0.837$
Hydroxytyrosol	1.87	0.970	$y = 0.0592x - 1.0586$
Low-OL	2.32	0.986	$y = 0.0549x - 0.4273$
Mid-OL	2.81	0.960	$y = 0.0666x - 0.5215$
High-OL	1.72	0.981	$y = 0.0562x - 1.0903$

Abbreviations: glu, glucoside; IC$_{50}$, half maximal inhibitory concentration; OL, olive leaf.

In terms of inflammation, elevated COX-2 expression in AD patients correlates with disease severity. The high-OL extract demonstrated the lowest IC$_{50}$ for COX-2 inhibition, surpassing hydroxytyrosol alone (Table 2). Interestingly, hydroxytyrosol exhibited robust COX-2 inhibitory activity, consistent with previous findings in cell lines and rodents (Fuccelli et al. 2018; Scoditti et al. 2014; Yonezawa et al. 2019; Zhang et al. 2009). Oleuropein displayed a lower IC$_{50}$ for COX-2 inhibition but is known for its anti-inflammatory effects in rodents and humans, highlighting a potential limitation of in vitro testing (Giner et al. 2011; W.-C. Huang et al. 2022; Larussa et al. 2017).

3.3 | Effect of the Three-OL Extracts on Amyloid-*β* Metabolism in *C. elegans*

A*β*-induced toxicity tolerance tests were performed using transgenic strains CL4176 and CL802. CL4176 expresses human A*β*$_{1–42}$ peptide, leading to paralysis, whereas CL802 serves as a negative control. The OL extracts demonstrated effectiveness in delaying amyloidogenic toxicity. The mid-OL extract exhibited the lowest protective effect, whereas low- and high-OL extracts had similar modulatory activities (Figure 1A). Thioflavin T staining confirmed these results, with the mid-OL extract showing more A*β* aggregates, whereas the extremes presented lower or no accumulation (Figure 1B). The anti-amyloidogenic toxicity activity of OL extracts was linked to reduced A*β* aggregation in treated nematodes, consistent with previous studies on olive by-products (Romero-Márquez et al. 2022b; Romero-Márquez et al. 2022a). A plausible hypothesis is that the modulatory effect exerted by OL extracts might be attributed, at least in part, to the overall phytochemical content. In this scenario, once the OL extract achieves a therapeutical phytochemical content, the individual contributions may take a secondary role in the general effect. To mention, high-OL extract demonstrated the lowest A*β* aggregation, which could be attributed to the overall TPC and TFC as well as the elevated oleuropein content (Diomede
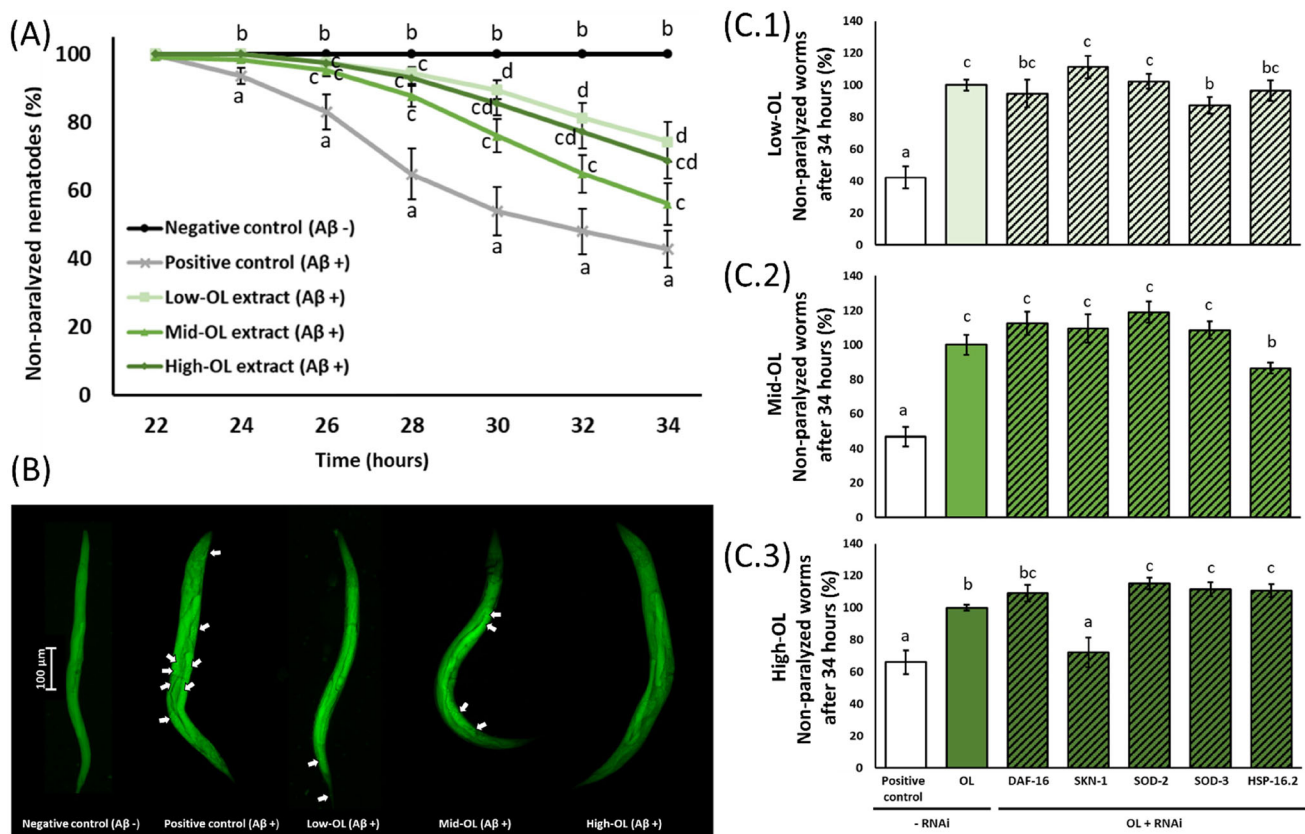
FIGURE 1 | Effects of the three OL extracts at 500 µg/mL on amyloid-β metabolism in *Caenorhabditis elegans*. (A) Paralysis phenotype. (B) Representative images of the thioflavin T staining in CL4176 and CL802 nematodes collected 28 h after the temperature upshift. (C) Influence of the different RNAi (DAF-16, SKN-1, SOD-2, SOD-3, and HSP-16.2) in the transgenic strain CL4176 at 34 h after the temperature upshift. (C.1) Low-OL extract; (C.2) mid-OL extract; (C.3) high-OL extract. *Note:* (A) For each time, different letters between experimental groups mean statistically significant differences ($p < 0.05$). (B) Pictures were taken at 10× magnification. White arrow shows the aggregated Aβ. (C) For each chart, different letters between experimental groups mean statistically significant differences ($p < 0.05$). Results are expressed as mean ± SEM. Aβ, amyloid-β; DAF, abnormal dauer formation; HSP, heat shock protein; OL, olive leaf; SKN, skinhead; SOD, superoxide dismutase.

et al. 2013; Luccarini et al. 2014; Rigacci et al. 2011). However, both low- and mid-OL extracts achieved a similar therapeutic effect. Different epidemiological studies have demonstrated that once an optimal therapeutic phytochemical intake is reached, no further benefits are observed at histological levels (Delshad Aghdam et al. 2021; Hamedi-Shahraki et al. 2023; Kim and Park 2022; Mirzababaei et al. 2022). Indeed, when the intake of phytochemical-rich plant-based food is adjusted in the regression analysis, amyloid imaging biomarkers have been shown to be modulated in this manner (Vassilaki et al. 2018).

To understand the mechanisms underlying OL extract effects on Aβ peptide toxicity, RNAi technology was used, targeting DAF-16/FOXO and SKN-1/NRF-2 pathways. Low-OL extract showed a dependency on the *SOD-3* gene, linked to a lower Aβ-plaque deposition (Figure 1C.1) (Bitner et al. 2012; Massaad et al. 2009). Mid-OL extract exhibited protective effects through the modulation of the proteostasis network (Figure 1C.2), possibly related to the induction of DAF-16/FOXO and HSP-16.2 due to its high content of apigenin derivatives (Elkhedir et al. 2022). The most intriguing outcomes emerged from high-OL extract treatment, where the SKN-1/NRF-2 pathway was involved. The inhibition of SKN-1/NRF-2 generated the total abolishment of the effectiveness of high-OL extract. Conversely, the individual inhibition of

both MnSODs, SOD-2 and SOD-3, enhanced the effectiveness of high-OL extract (Figure 1C.3). In this context, SKN-1/NRF-2 encodes both SOD-2 and SOD-3 gene expressions. SOD-2 encodes the major MnSOD mitochondrial isoforms, whereas SOD-3 encodes auxiliary and inducible ones in *C. elegans*. When SOD-2 is knocked out, an overcompensation of SOD-3 production occurs, and vice versa (Van Raamsdonk and Hekimi 2009). This heightened production of SOD enzymes contributes to the improvement of the therapeutic effect induced by the high-OL extract, which has been related to a reduction of AD markers in rodents (Bitner et al. 2012; Massaad, Washington, et al. 2009) and in *C. elegans* (Romero-Márquez et al. 2022a). Knocking down HSP-16.2 also increased the effectiveness, implying an interaction between HSP-16.2 and the antioxidant response element (ARE) system (Hartwig et al. 2009; Strayer et al. 2003).

3.4 | Effect of the Three-OL Extracts on Hyperphosphorylated Tau Protein Metabolism

Tau-induced neurotoxicity was evaluated in the present study in the *C. elegans* strain BR5706 expressing pro-aggregative human tau by assessing locomotion defects. Low- and high-OL extracts effectively mitigated tau-associated neurotoxicity, whereas the
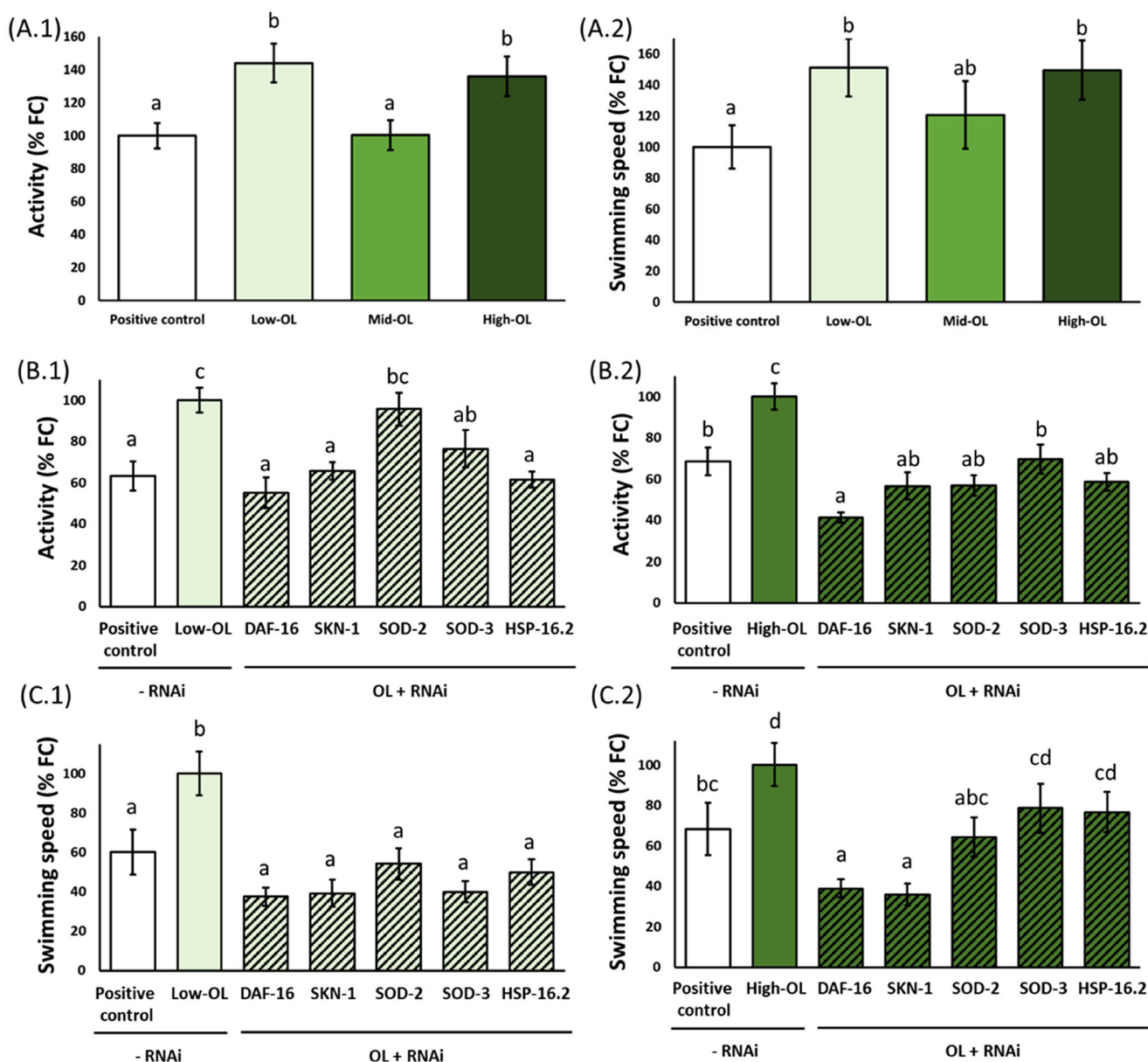
FIGURE 2 | **Effects of the three OL extracts on hyperphosphorylated tau protein metabolism in *Caenorhabditis elegans*.** (A) Effects of the three olive leaf extracts at 500 μg/mL on locomotive parameters in the transgenic strain BR5706; (B) effects of the low- and high-OL extract at 500 μg/mL on activity in the transgenic strain BR5706 and the influence of the different RNAi; (C) effects of the low- and high-OL extract at 500 μg/mL on swimming speed in the transgenic strain BR5706 and the influence of the different RNAi. DAF, abnormal dauer formation; HSP, heat shock protein; FC, fold change; OL, olive leaf; SKN, skinhead; SOD, superoxide dismutase.

mid-OL extract was not effective in preventing tau protein expression (Figure 2A).

To elucidate mechanisms underlying the effects of low- and high-OL extracts, RNAi technology was applied. In low-OL extract–treated nematodes, DAF-16/FOXO, SKN-1/NRF-2, and HSP-16.2. RNAi resulted in the abolition of therapeutic effects, suggesting the involvement of these pathways in the action mechanism of the extract (Figure 2B.1,C.1). Similarly, nematodes treated with high-OL extract and subjected to DAF-16/FOXO or SKN-1/NRF-2 RNAi also exhibited a loss of therapeutic effects (Figure 2B.2,C.2).

Evidence on the role of olive by-products in tauopathies is limited. However, studies using olive by-products enriched in oleuropein

40% (O-OL) and hydroxytyrosol 20% (H-OF) in a *C. elegans* model of tauopathy revealed similar therapeutic effects. In fact, 40% O-OL extract demonstrated its modulatory effects through DAF-16/FOXO, SKN-1/NRF-2, and HSP-16.2 (Romero-Márquez et al. 2022a). These transcription factors are key regulators of antioxidant, xenobiotic, and stress responses, and their inhibition disrupts downstream targets such as SOD and HSP-16.2, which play significant roles in tauopathy mitigation in *C. elegans* (Tullet et al. 2017). Common components in 40% O-OL and high-OL extracts, such as secoiridoids and phenolic acids, exhibit mitohormetic effects by upregulating the SKN-1/NRF-2 signaling pathway and modulating mitochondrial function (Blackwell et al. 2015; Menendez et al. 2013; Romero-Márquez et al. 2022b). Individual compounds in high-OL extract, including oleuropein
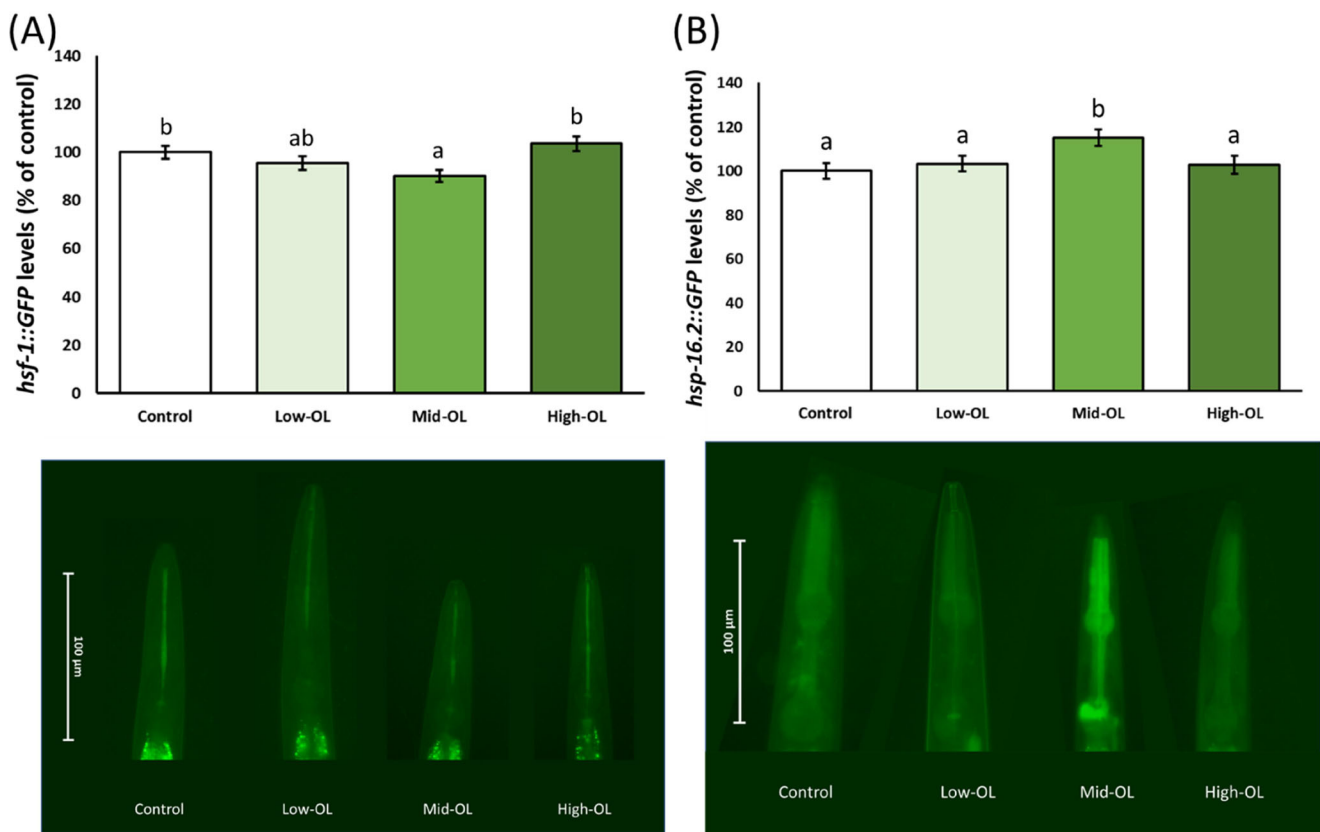
FIGURE 3 | Effects of the three olive leaf extracts at 500 µg/mL on (A) TJ356/DAF-16p::GFP strain, (B) LD1/SKN-1::GFP strain. HSF, heat shock factor; HSP, heat shock protein; OL, olive leaf.

and hydroxytyrosol derivatives, have been shown to interfere with tau fibrillization and aggregation at low dosages, offering promise for mitigating tau toxicity (Daccache et al. 2011).

3.5 | Effect of the Three-OL Extracts on Components of the Antioxidant and Proteostasis Network in *C. elegans*

Transgenic strain OS3062 was used to explore the impact of OL extracts on the HSF-1 pathway. Treatment with low- and high-OL extracts did not alter basal HSF-1 levels, whereas mid-OL extract led to a lower expression in this transcription factor compared to the control group (Figure 3A). Limited research on OL extract's role in the HSF-1 pathway exists, with Feng et al. (2021) demonstrating increased HSF-1 mRNA levels using isolated oleuropein (Feng et al. 2021). However, the concentration used was impractical with realistic OL extract doses. In the TJ375 strain, 500 µg/mL of low- and high-OL extracts did not affect basal HSP-16.2 levels, whereas mid-OL extract led to higher HSP-16.2 expression than in control group (Figure 3B). Three studies evaluated the impact of olive by-products on HSP-16.2 levels using the TJ375 strain. All treatments led to higher expression in this strain, which was attributed to hormetic mechanisms related to high hydroxytyrosol and oleuropein content (Luo et al. 2019; Romero-Márquez et al. 2022b; Romero-Márquez et al. 2022a).

To investigate the impact of OL extracts on the DAF-16/FOXO pathway, the transgenic strain TJ356 was analyzed. Results revealed that treatment with 500 µg/mL of all OL extracts resulted

in higher values for nucleation of DAF-16/FOXO compared to the control, indicating that the dose was sufficient to induce DAF-16/FOXO in all treatments (Figure 4A). This aligns with Luo et al. (2019), who demonstrated increased nuclear distribution of DAF-16/FOXO in TJ356 nematodes treated with 400 µg/mL of methanolic OL extract (Luo et al. 2019). This correlation aligns with the higher levels of HSP-16.2 observed in nematodes treated with mid-OL extract in the TJ375 strain, suggesting a potential link between DAF-16/FOXO induction and proteostasis modulation. The association between DAF-16/FOXO and HSP-16.2 induction by mid-OL is supported by the extract's high content of apigenin derivatives, which has been shown to enhance DAF-16/FOXO translocation and induce HSP-16.2 in *C. elegans* (Elkhedir et al. 2022). Interestingly, the induction of DAF-16/FOXO and HSP-16.2 by the mid-OL extract, along with their subsequent protective effects, might be attributed to a potential side effect, as high concentrations of isolated apigenin derivatives have demonstrated non-lethal toxic effects through DAF-16/FOXO/HSP-16.2 modulation in *C. elegans* (Kawasaki et al. 2010).

The SKN-1/NRF-2 transcription factor was assessed using the transgenic strain LD1. Treatment with 500 µg/mL of low- and high-OL extracts resulted in higher SKN-1/NRF-2 expression, whereas mid-OL did not alter the levels (Figure 4B). These findings align with the results observed in the present study concerning amyloid and p-tau assays, indicating that modulatory activity of mid-OL extract is mainly attributed to proteostasis network modulation mediated by DAF-16/FOXO and HSF-1.
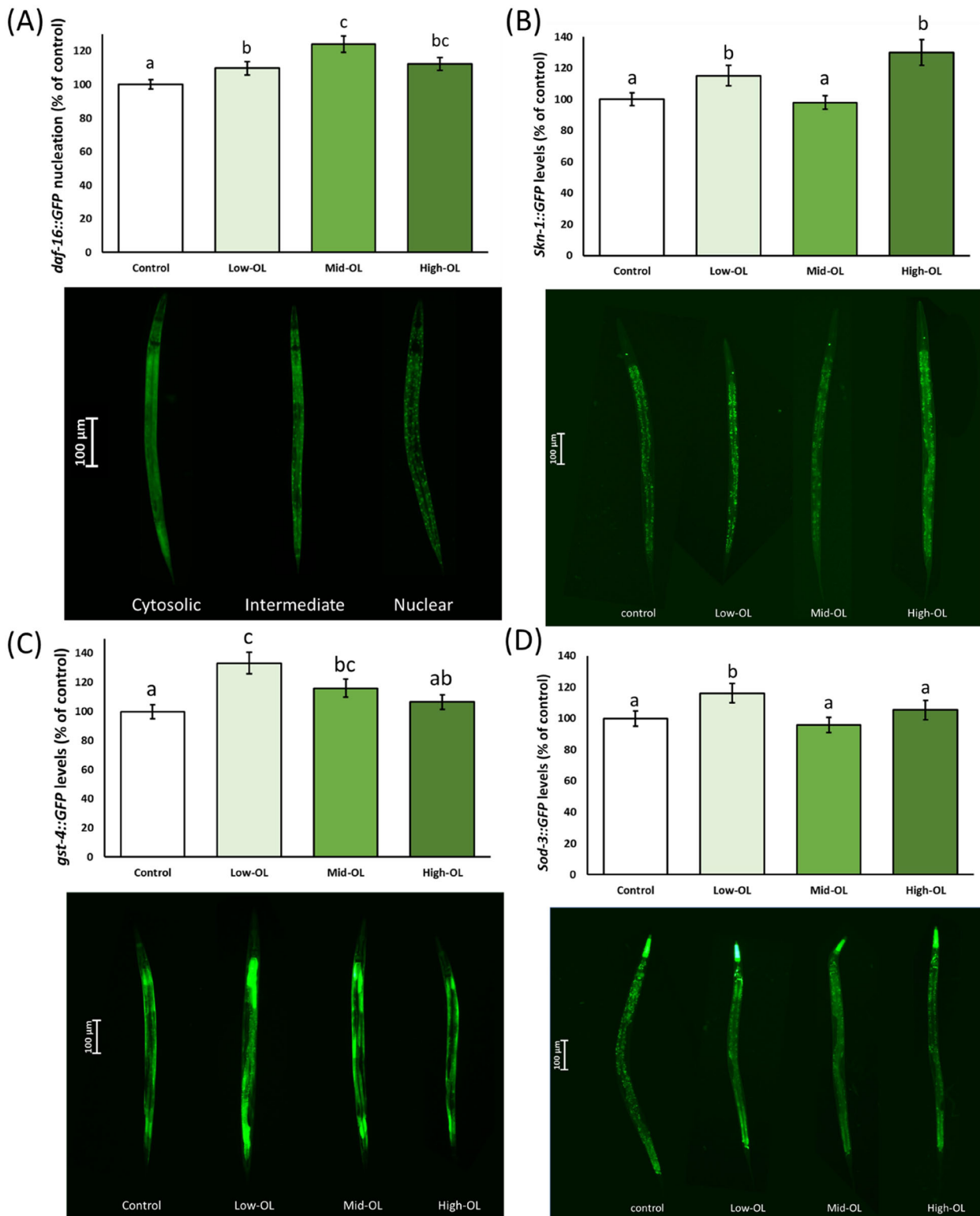
FIGURE 4 | Effects of the three olive leaf extracts at 500 µg/mL on (A) OS3062/hsf-1::GFP strain, (B) CL2166/GST-4p::GFP strain, (C) CF1553/sod-3p::GFP, (D–F) TJ375/hsp-16.2p::GFP. DAF, abnormal dauer formation; GST, glutathione S transferase; HSF, heat shock factor; HSP, heat shock protein; OL, olive leaf; SKN, skinhead; SOD, superoxide dismutase.

The differential effect of mid-OL on SKN-1/NRF-2 compared to DAF-16/FOXO suggests a differential regulatory response to OL extracts. Notably, the high-OL extract induced the highest SKN-1/NRF-2 levels (23%), potentially linked to its high content of secoiridoids, which have been shown to induce mitohormetic effects by upregulating the SKN-1/NRF-2 signaling pathway and modulating mitochondrial function in *C. elegans* (Blackwell et al. 2015; Menendez et al. 2013). These findings are consistent with the results obtained in the present study in the experiments involving amyloid and p-tau, which emphasized

the pivotal role of SKN-1/NRF-2 and the major mitochondrial MnSOD, SOD-2, in the health benefits conferred by the high-OL extract.

To assess the impact of OL extracts on SOD-3 levels, the transgenic strain CF1553 was utilized. Among the OL extracts studied, only the treatment with 500 μg/mL of low-OL extract induced basal levels of SOD-3 (Figure 4D). The absence of an effect from mid- and high-OL extracts on SOD-3 suggests that the protective effects of mid-OL are primarily mediated through proteostasis modulation, whereas high-OL might be involved in ARE system modulation, potentially through SOD-2. The isoform-specific effects hint at the importance of phytochemical composition in influencing outcomes.

The effect of OL extracts on GST-4, a cytosolic enzyme in phase II detoxification, was assessed using the transgenic strain CL2166. Among the OL extracts studied, only the treatment with 500 μg/mL of low- and mid-OL extracts showed higher levels of GST-4, with the greatest induction observed for low-OL (25%) (Figure 4C). The absence of an increase in GST-4 levels with the high-OL extract could be attributed to its strong antioxidant activity, particularly as a free radical scavenger, mainly due to the elevated content of oleuropein and its derivatives. In vitro studies have shown that several ROS scavengers can reduce the expression or activity of inducible antioxidant enzymes such as GST (Jin et al. 2016). This feature has been demonstrated in randomized double-blind trials, reporting that the intake of oleuropein-rich extra virgin olive oil enhanced plasma GSH and reduced the activity of GSH peroxidase (GSH-Px) (Oliveras-López et al. 2013; Perez-Herrera et al. 2013).

3.6 | Effect of the Three-OL Extracts on Redox Biology During Aβ Pathology

To evaluate the impact of OL extracts in preventing Aβ-induced oxidative stress, intracellular ROS levels were measured in an amyloidogenic *C. elegans* model. The CL4176 strain was employed, modeling oxidative damage prior to Aβ-plaque deposition. $A\beta_{1-42}$ production in the positive control led to significantly higher intracellular ROS content compared to the negative control (Figure 4A), consistent with oxidative damage preceding Aβ aggregation in early AD (Drake et al. 2003; Nunomura et al. 2006).

All OL extract treatments partially prevented intracellular ROS formation in CL4176 nematodes (Figure 5A). The low-OL extract exhibited the greatest preventive effect compared to the positive control, potentially linked to a 25% increase in GST-4 expression. GST-4 catalyzes the conjugation of GSH to xenobiotic substrates for detoxification, contributing to reduced intracellular ROS content (Ferguson and Bridge 2019). Similarly, the mid-OL extract demonstrated a 73% reduction in intracellular ROS, suggesting the involvement of GST-4 and HSP-16.2 overproduction in this potential effect.

The nematodes treated with high-OL extract exhibited a 77% lower ROS level compared to control, despite unaltered GST-4 levels. This result could be associated with the influence of high-OL extract on SOD-2, a major mitochondrial MnSOD isoform in *C. elegans* known for its significant contribution to oxidative

stress amelioration in the presence of amyloid pathology (Bitner et al. 2012; Massaad et al. 2009; Massaad, Washington, et al. 2009). Additionally, the potent free radical scavenging activity of high-OL extract, attributed to its secoiridoid content, may contribute to the lower ROS formation (Rietjens et al. 2007; Umeno et al. 2015).

On the other hand, decreased levels of mitochondrial enzymes coupled with increased oxidized iron and biomolecules elevate oxidative stress within mitochondria (Bosetti et al. 2002; Parker et al. 1994; Smith et al. 1997; Youssef et al. 2018). Aβ oligomers further exacerbate mitochondrial dysfunction, disrupting electron transport chain complexes and amplifying ROS production (Chen et al. 2022; Onukwufor et al. 2022). To assess the impact of OL extracts on Aβ-induced oxidative stress at the mitochondrial level, the MitoTracker Red CM-H$_2$XRos dye was employed in an amyloidogenic *C. elegans* model. $A\beta_{1-42}$ production in the positive control intensified mitochondrial ROS content (Figure 5B), aligning with literature highlighting Aβ-induced mitochondrial dysfunction and increased ROS levels (Hawking 2016; Picone et al. 2014). High-OL extract–treated nematodes exhibited lower mitochondrial ROS content than the positive control (Figure 4B), consistent with RNAi experiments showing a modulatory effect through mitochondrial MnSODs. A potential mitohormetic effect of high-OL extract may prime the antioxidant response, inducing SOD overcompensation, particularly SOD-2. The secoiridoids in high-OL extract might be implicated in upregulating the SKN-1/NRF-2 pathway and modulating mitochondrial function in *C. elegans*. Additionally, due to the high FRAP activity reported, high-OL extract may reduce the oxidized iron pool, preventing its binding to Aβ oligomers and preserving electron transport chain complexes in the mitochondrial membrane (Onukwufor et al. 2022). The decrease in oxidized iron levels may further contribute to reduced hydroxyl radicals and oxidized biomolecules, helping in oxidative stress amelioration (Zhao 2019). This aligns with findings demonstrating that oleuropein-rich OL extract improved iron homeostasis and mitochondrial functions in hematopoietic stem cells (Kondo et al. 2021). In contrast, both low- and mid-OL extracts did not influence mitochondrial ROS content in the amyloidogenic strain. These extracts modulated GSH metabolism through GST-4, primarily located in the cytosol. Overproduction of GST-4 might reduce intracellular ROS but not mitochondrial ones.

Finally, GSH levels were measured in an amyloidogenic *C. elegans* model. High-OL extract treatment led to a significantly higher GSH content, showing similar levels to those found in the negative control (Figure 5C). In contrast, low- and mid-OL extracts did not alter GSH levels. The unaltered GSH content in low- and mid-OL extracts may be attributed to heightened GST-4 overexpression, suggesting GSH consumption for xenobiotic detoxification rather than an absence of extract effects. These results are supported by the low FRAP values for low- and mid-OL extracts, which might support an increased GSH utilization to counteract oxidative stress. The distinctive effect of high-OL extract in countering oxidative stress might be attributed to its potent free radical scavenger activity, chelation of oxidized iron, and prevention of mitochondrial ROS production. GSH plays a vital role in chelating cytoplasmic free iron during amyloid pathology, preventing uncontrolled redox reactions (Mandal et al. 2022). The high iron-reducing antioxidant capacity of high-OL
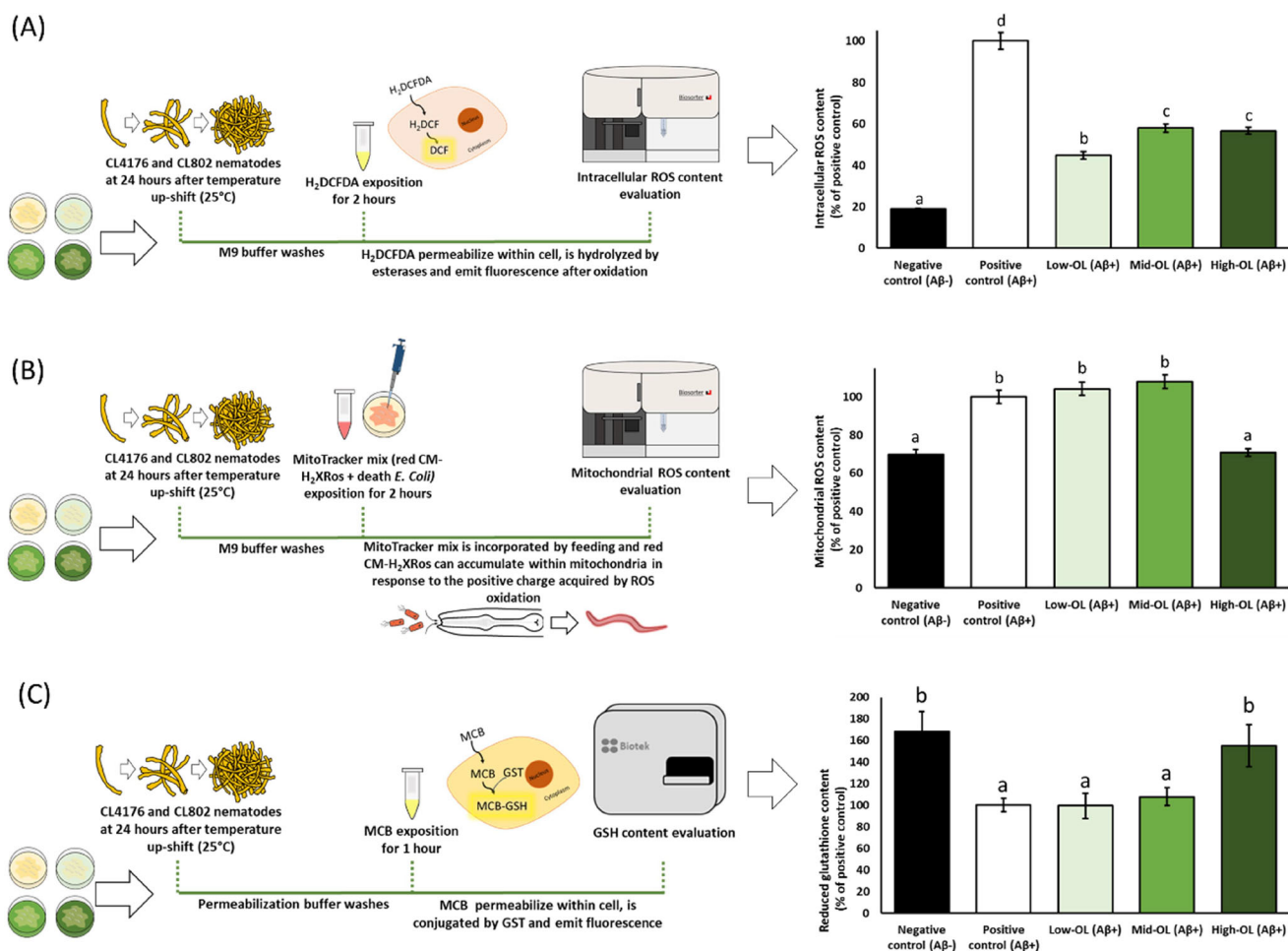
FIGURE 5 | Intracellular and mitochondrial ROS content and GSH levels in *Caenorhabditis elegans* expressing Amyloid β1–42 peptide treated or not with three different OL extracts at 24 h after temperature up-shift: (A) intracellular ROS content; (B) mitochondrial ROS content; (C) reduced glutathione content. DCF, dichlorofluorescein; GSH, glutathione; GST, glutathione S-transferase; MCB, monochlorobimane; OL, olive leaf; ROS, reactive oxygen species.

extract, coupled with SOD-2 involvement, may reduce GSH consumption for binding oxidized molecules, resulting in reduced GST-4 expression and the preservation of high GSH levels. A limitation of the study is the focus on total reduced GSH content and GST-4 levels without evaluating oxidized GSSG, GSH/GSSG ratio, or GSSG reductases. Further research is needed to confirm the proposed hypothesis.

3.7 | Effect of the Three-OL Extracts on Redox Biology During Tauopathy

To explore the impact of low- and high-OL extracts on p-tau-induced oxidative stress, intracellular ROS levels were measured in the tauopathy strain of *C. elegans* using the H$_2$DCFDA dye method. Surprisingly, both low- and high-OL extracts failed to prevent intracellular ROS accumulation compared to the positive control (Figure 6A). Evidence regarding the role of OL extract in mitigating p-tau neurotoxicity is scarce, and its ability to modulate oxidative stress in tauopathy has not been thoroughly evaluated. In the present research, both low- and high-OL extracts significantly reduced mitochondrial ROS accu-

mulation when compared to positive control (Figure 6B). These results correlated with heightened SOD-2 involvement in RNAi experiments.

Finally, the impact of low- and high-OL extracts on GSH content in a *C. elegans* tauopathy model was investigated (Figure 5C). Results revealed that both low- and high-OL extracts led to a higher GSH content compared with control group. These results agreed with what was observed concerning mitochondrial ROS levels, as exposed above. Intriguingly, the low-OL extract exhibited the highest GSH content in the tauopathy strain, contrasting with the amyloidogenic strain's findings. The protective effects in the tauopathy strain were associated with SOD-2 and HSP-16.2 involvement, influencing GSH levels and antioxidative effects. However, the high-OL extract–treated nematodes showed lower GSH content, potentially due to robust SOD-2 engagement in preventing mitochondrial ROS production. This observation is consistent with the reduced mitochondrial ROS levels, which are accompanied by decreased GSH levels in both strains, indicating a potential link between oxidative stress reduction and GSH content. Thus, the present study suggests a connection between SOD-2 involvement, mitochondrial ROS reduction, and GSH content changes (Von Montfort et al. 2012), emphasizing the
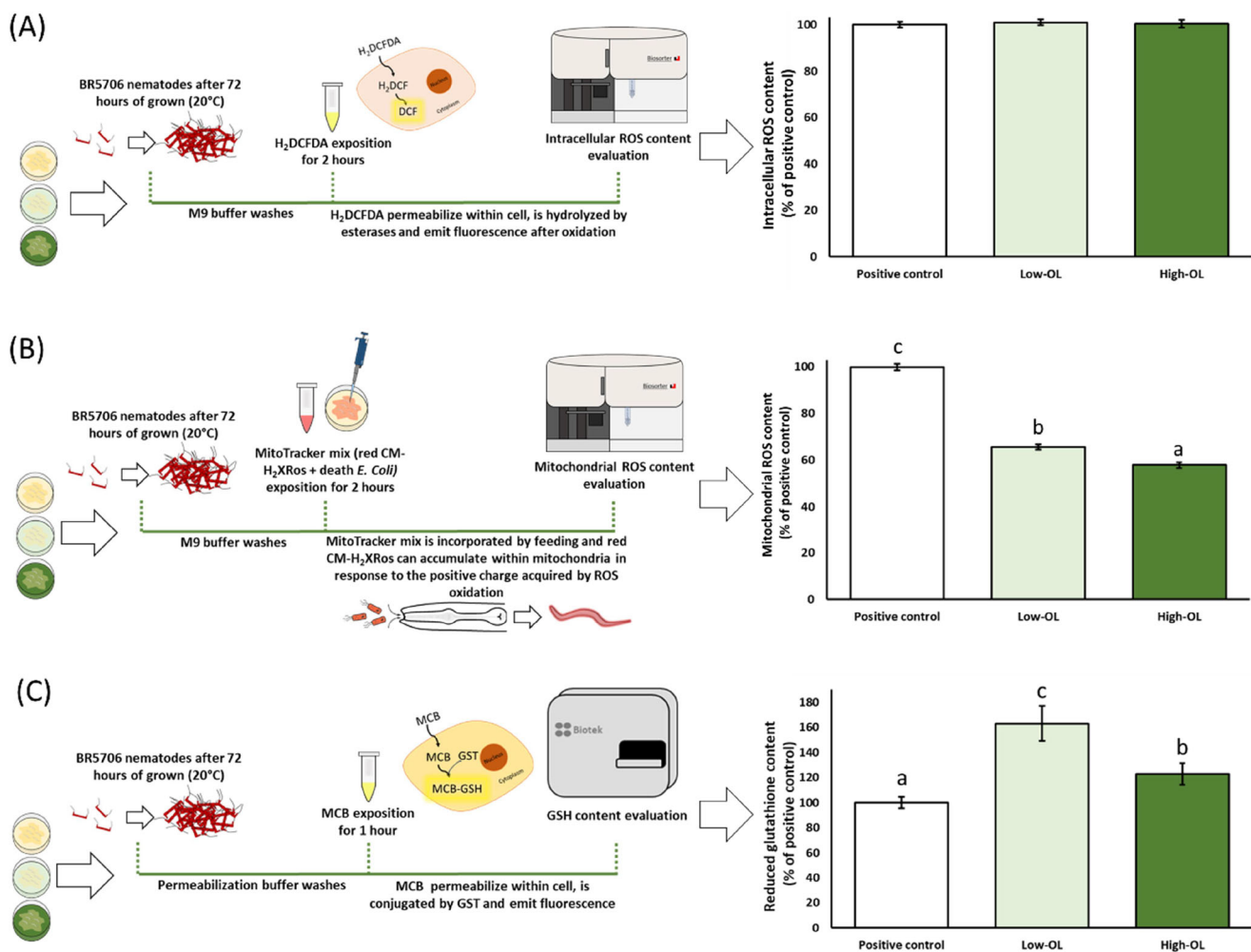
FIGURE 6 | Intracellular and mitochondrial ROS content and GSH levels in *Caenorhabditis elegans* expressing phosphorylated tau protein treated or not with two different OL extracts at 24 h after temperature up-shift: (A) intracellular ROS content; (B) mitochondrial ROS content; (C) reduced glutathione content. DCF, dichlorofluorescein; GST, glutathione S-transferase; MCB, monochlorobimane; GSH, glutathione; OL, olive leaf; ROS, reactive oxygen species.

significant role of SOD-2 in the protective effects of high-OL extract in the tauopathy model.

4 | Conclusions

The present study investigated OL extracts, emphasizing their anti-inflammatory, anti-cholinergic, and antioxidant capacity in vitro. The three OL extracts demonstrated significant anti-inflammatory, anti-cholinergic, and iron-reducing activities. The study also evaluated the impact of low-, mid-, and high-OL extracts on Aβ and tau proteotoxicity in vivo. Although mid-OL only showed slight improvement in amyloidogenic toxicity, both low- and high-OL extracts exhibited notable benefits. Involvement of transcription factors SKN-1/NRF-2, along with downstream SOD-2 and SOD-3, was evident in low- and high-OL extract effects, with HSP-16.2 contributing to mid-OL benefits. The three extracts modulated redox biology, probably via hormetic stress responses, inducing DAF-16/FOXO nucleation. In the presence of amyloidogenic pathology, all extracts effectively prevented intracellular ROS excess, with low-OL being the most active. Protective effects on GSH metabolism involved GST-

4, HSP-16.2, and SOD-2 for low-, mid-, and high-OL extracts, respectively. Only the high-OL extract prevented ROS accumulation at the mitochondrial level, implicating SOD-2. In hyperphosphorylated tau strains, both low- and high-OL extracts partially prevented mitochondrial ROS accumulation through DAF-16/SKN-1, SOD-2, and SOD-3. Overall, these results endorse that, at least in part, the effects of the three OL extracts on AD are exerted through the modulation of redox biology, although additional pathways could also be involved. In addition, these observations and mechanisms open the door for the design and testing of nutraceuticals based on OL extracts aimed at preventing or mitigating various aspects related to AD.

Conflicts of Interest

The authors declare no conflicts of interest.

Data Availability Statement

The data that support the findings of this study are available from the corresponding author upon reasonable request. However, due to the ongoing nature of the publicly funded research project, data access may be subject to restrictions until the project is completed.

Ethics Statement

Ethical approval was not required for this study, as experiments involving *Caenorhabditis elegans* are not subject to evaluation by ethics committees under both European (Directive 2010/63/EU) and Spanish (RD 53/2013) legislation.

References

Alcántara, C., T. Žugčić, R. Abdelkebir, et al. 2020. "Effects of Ultrasound-Assisted Extraction and Solvent on the Phenolic Profile, Bacterial Growth, and Anti-Inflammatory/Antioxidant Activities of Mediterranean Olive and Fig Leaves Extracts." *Molecules (Basel, Switzerland)* 25, no. 7: Article 7. https://doi.org/10.3390/molecules25071718.

Bitner, B. R., C. J. Perez-Torres, L. Hu, T. Inoue, and R. G. Pautler. 2012. "Improvements in a Mouse Model of Alzheimer's Disease Through Sod2 Overexpression Are Due to Functional and Not Structural Alterations." *Magnetic Resonance Insights* 5: MRI.S9352. https://doi.org/10.4137/MRI.S9352.

Blackwell, T. K., M. J. Steinbaugh, J. M. Hourihan, C. Y. Ewald, and M. Isik. 2015. "SKN-1/Nrf, Stress Responses, and Aging in *Caenorhabditis elegans*." *Free Radical Biology & Medicine* 88, no. pt B: 290–301. https://doi.org/10.1016/j.freeradbiomed.2015.06.008.

Bosetti, F., F. Brizzi, S. Barogi, et al. 2002. "Cytochrome c Oxidase and Mitochondrial F1F0-ATPase (ATP Synthase) Activities in Platelets and Brain From Patients With Alzheimer's Disease." *Neurobiology of Aging* 23, no. 3: 371–376. https://doi.org/10.1016/s0197-4580(01)00314-1.

Chen, Z.-R., J.-B. Huang, S.-L. Yang, and F.-F. Hong. 2022. "Role of Cholinergic Signaling in Alzheimer's Disease." *Molecules (Basel, Switzerland)* 27, no. 6: Article 6. https://doi.org/10.3390/molecules27061816.

Daccache, A., C. Lion, N. Sibille, et al. 2011. "Oleuropein and Derivatives From Olives as Tau Aggregation Inhibitors." *Neurochemistry International* 58, no. 6: 700–707. https://doi.org/10.1016/j.neuint.2011.02.010.

Davies, P., and A. J. Maloney. 1976. "Selective Loss of Central Cholinergic Neurons in Alzheimer's Disease." *Lancet (London, England)* 2, no. 8000: 1403. https://doi.org/10.1016/s0140-6736(76)91936-x.

Delshad Aghdam, S., F. Siassi, E. Nasli Esfahani, et al. 2021. "Dietary Phytochemical Index Associated With Cardiovascular Risk Factor in Patients With Type 1 Diabetes Mellitus." *BMC Cardiovascular Disorders* 21, no. 1: 293. https://doi.org/10.1186/s12872-021-02106-2.

Diomede, L., S. Rigacci, M. Romeo, M. Stefani, and M. Salmona. 2013. "Oleuropein Aglycone Protects Transgenic *C. elegans* Strains Expressing Aβ42 by Reducing Plaque Load and Motor Deficit." *PLoS ONE* 8, no. 3: e58893. https://doi.org/10.1371/journal.pone.0058893.

Drake, J., C. D. Link, and D. A. Butterfield. 2003. "Oxidative Stress Precedes Fibrillar Deposition of Alzheimer's Disease Amyloid Beta-Peptide (1–42) in a Transgenic *Caenorhabditis elegans* Model." *Neurobiology of Aging* 24, no. 3: 415–420. https://doi.org/10.1016/s0197-4580(02)00225-7.

Elkhedir, A. E., A. Iqbal, D. Zogona, H. H. Mohammed, A. Murtaza, and X. Xu. 2022. "Apigenin Glycosides From Green Pepper Enhance Longevity and Stress Resistance in *Caenorhabditis elegans*." *Nutrition Research* 102: 23–34. https://doi.org/10.1016/j.nutres.2022.02.003.

Ellman, G. L., K. D. Courtney, V. Andres, and R. M. Feather-Stone. 1961. "A New and Rapid Colorimetric Determination of Acetylcholinesterase Activity." *Biochemical Pharmacology* 7: 88–95. https://doi.org/10.1016/0006-2952(61)90145-9.

Everett, J., J. F. Collingwood, V. Tjendana-Tjhin, et al. 2018. "Nanoscale Synchrotron X-Ray Speciation of Iron and Calcium Compounds in Amyloid Plaque Cores From Alzheimer's Disease Subjects." *Nanoscale* 10, no. 25: 11782–11796. https://doi.org/10.1039/C7NR06794A.

Feng, S., C. Zhang, T. Chen, et al. 2021. "Oleuropein Enhances Stress Resistance and Extends Lifespan via Insulin/IGF-1 and SKN-1/Nrf2 Signaling Pathway in *Caenorhabditis elegans*." *Antioxidants* 10, no. 11: Article 11. https://doi.org/10.3390/antiox10111697.

Ferguson, G. D., and W. J. Bridge. 2019. "The Glutathione System and the Related Thiol Network in *Caenorhabditis elegans*." *Redox Biology* 24: 101171. https://doi.org/10.1016/j.redox.2019.101171.

Fuccelli, R., R. Fabiani, and P. Rosignoli. 2018. "Hydroxytyrosol Exerts Anti-Inflammatory and Anti-Oxidant Activities in a Mouse Model of Systemic Inflammation." *Molecules (Basel, Switzerland)* 23, no. 12: 3212. https://doi.org/10.3390/molecules23123212.

Giner, E., I. Andújar, M. C. Recio, J. L. Ríos, J. M. Cerdá-Nicolás, and R. M. Giner. 2011. "Oleuropein Ameliorates Acute Colitis in Mice." *Journal of Agricultural and Food Chemistry* 59, no. 24: 12882–12892. https://doi.org/10.1021/jf203715m.

Godos, J., G. L. Romano, S. Laudani, et al. 2024. "Flavan-3-Ols and Vascular Health: Clinical Evidence and Mechanisms of Action." *Nutrients* 16, no. 15: Article 15. https://doi.org/10.3390/nu16152471.

Guan, P.-P., X. Yu, Y.-H. Zou, and P. Wang. 2019. "Cyclooxygenase-2 Is Critical for the Propagation of β-Amyloid Protein and Reducing the Glycosylation of Tau in Alzheimer's Disease." *Cellular & Molecular Immunology* 16, no. 11: Article 11. https://doi.org/10.1038/s41423-019-0294-1.

Hamedi-Shahraki, S., M.-R. Jowshan, M.-A. Zolghadrpour, F. Amirkhizi, and S. Asghari. 2023. "Dietary Phytochemical Index Is Favorably Associated With Oxidative Stress Status and Cardiovascular Risk Factors in Adults With Obesity." *Scientific Reports* 13: 7035. https://doi.org/10.1038/s41598-023-34064-4.

Hartwig, K., T. Heidler, J. Moch, H. Daniel, and U. Wenzel. 2009. "Feeding a ROS-Generator to *Caenorhabditis elegans* Leads to Increased Expression of Small Heat Shock Protein HSP-16.2 and Hormesis." *Genes & Nutrition* 4, no. 1: 59–67. https://doi.org/10.1007/s12263-009-0113-x.

Hawking, Z. L. 2016. "Alzheimer's Disease: The Role of Mitochondrial Dysfunction and Potential New Therapies." *Bioscience Horizons: The International Journal of Student Research* 9: hzw014. https://doi.org/10.1093/biohorizons/hzw014.

Ho, L., C. Pieroni, D. Winger, D. P. Purohit, P. S. Aisen, and G. M. Pasinetti. 1999. "Regional Distribution of Cyclooxygenase-2 in the Hippocampal Formation in Alzheimer's Disease." *Journal of Neuroscience Research* 57, no. 3: 295–303. https://doi.org/10.1002/(SICI)1097-4547(19990801)57:3⟨295::AID-JNR1⟩3.0.CO;2-0.

Ho, L., D. Purohit, V. Haroutunian, et al. 2001. "Neuronal Cyclooxygenase 2 Expression in the Hippocampal Formation as a Function of the Clinical Progression of Alzheimer Disease." *Archives of Neurology* 58, no. 3: 487–492. https://doi.org/10.1001/archneur.58.3.487.

Huang, D., B. Ou, and R. L. Prior. 2005. "The Chemistry Behind Antioxidant Capacity Assays." *Journal of Agricultural and Food Chemistry* 53, no. 6: 1841–1856. https://doi.org/10.1021/jf030723c.

Huang, W.-C., C.-J. Liou, and S.-C. Shen. 2022. "Oleuropein Attenuates Inflammation and Regulates Immune Responses in a 2,4-Dinitrochlorobenzene-Induced Atopic Dermatitis Mouse Model." *Asian Pacific Journal of Allergy and Immunology*. https://doi.org/10.12932/AP-200122-1309.

in 't Veld, B. A., A. Ruitenberg, A. Hofman, et al. 2001. "Nonsteroidal Antiinflammatory Drugs and the Risk of Alzheimer's Disease." *New England Journal of Medicine* 345, no. 21: 1515–1521. https://doi.org/10.1056/NEJMoa010178.

Jin, C. H., Y. K. So, S. N. Han, and J.-B. Kim. 2016. "Isoegomaketone Upregulates Heme Oxygenase-1 in RAW264.7 Cells via ROS/p38 MAPK/Nrf2 Pathway." *Biomolecules & Therapeutics* 24, no. 5: 510–516. https://doi.org/10.4062/biomolther.2015.194.

Kawasaki, I., M.-H. Jeong, B.-K. Oh, and Y.-H. Shim. 2010. "Apigenin Inhibits Larval Growth of *Caenorhabditis elegans* Through DAF-16 Activation." *FEBS Letters* 584, no. 16: 3587–3591. https://doi.org/10.1016/j.febslet.2010.07.026.

Kim, C., and K. Park. 2022. "Association Between Phytochemical Index and Inflammation in Korean Adults." *Antioxidants* 11, no. 2: 348. https://doi.org/10.3390/antiox11020348.

Kondo, S., F. Ferdousi, K. Yamauchi, et al. 2021. "Comprehensive Transcriptome Analysis of Erythroid Differentiation Potential of Olive Leaf in Haematopoietic Stem Cells." *Journal of Cellular and Molecular Medicine* 25, no. 15: 7229–7243. https://doi.org/10.1111/jcmm.16752.

Lama-Muñoz, A., M. Contreras, M. del, et al. 2020. "Content of Phenolic Compounds and Mannitol in Olive Leaves Extracts From Six Spanish Cultivars: Extraction With the Soxhlet Method and Pressurized Liquids." *Food Chemistry* 320: 126626. https://doi.org/10.1016/j.foodchem.2020.126626.

Larussa, T., M. Oliverio, E. Suraci, et al. 2017. "Oleuropein Decreases Cyclooxygenase-2 and Interleukin-17 Expression and Attenuates Inflammatory Damage in Colonic Samples From Ulcerative Colitis Patients." *Nutrients* 9, no. 4: 391. https://doi.org/10.3390/nu9040391.

Luccarini, I., T. Ed Dami, C. Grossi, S. Rigacci, M. Stefani, and F. Casamenti. 2014. "Oleuropein Aglycone Counteracts Aβ42 Toxicity in the Rat Brain." *Neuroscience Letters* 558: 67–72. https://doi.org/10.1016/j.neulet.2013.10.062.

Luo, S., X. Jiang, L. Jia, et al. 2019. "In Vivo and In Vitro Antioxidant Activities of Methanol Extracts From Olive Leaves on *Caenorhabditis elegans*." *Molecules (Basel, Switzerland)* 24, no. 4: 704. https://doi.org/10.3390/molecules24040704.

Mandal, P. K., A. Goel, A. I. Bush, et al. 2022. "Hippocampal Glutathione Depletion With Enhanced Iron Level in Patients With Mild Cognitive Impairment and Alzheimer's Disease Compared With Healthy Elderly Participants." *Brain Communications* 4, no. 5: fcac215. https://doi.org/10.1093/braincomms/fcac215.

Massaad, C. A., R. G. Pautler, and E. Klann. 2009. "Mitochondrial Superoxide: A Key Player in Alzheimer's Disease." *Aging* 1, no. 9: 758–761. https://doi.org/10.18632/aging.100088.

Massaad, C. A., T. M. Washington, R. G. Pautler, and E. Klann. 2009. "Overexpression of SOD-2 Reduces Hippocampal Superoxide and Prevents Memory Deficits in a Mouse Model of Alzheimer's Disease." *Proceedings of the National Academy of Sciences of the United States of America* 106, no. 32: 13576–13581. https://doi.org/10.1073/pnas.0902714106.

McGeer, P. L., M. Schulzer, and E. G. McGeer. 1996. "Arthritis and Anti-Inflammatory Agents as Possible Protective Factors for Alzheimer's Disease: A Review of 17 Epidemiologic Studies." *Neurology* 47, no. 2: 425–432. https://doi.org/10.1212/wnl.47.2.425.

Menendez, J. A., J. Joven, G. Aragonès, et al. 2013. "Xenohormetic and Anti-Aging Activity of Secoiridoid Polyphenols Present in Extra Virgin Olive Oil." *Cell Cycle* 12, no. 4: 555–578. https://doi.org/10.4161/cc.23756.

Mirzababaei, A., A. Taheri, N. Rasaei, et al. 2022. "The Relationship Between Dietary Phytochemical Index and Resting Metabolic Rate Mediated by Inflammatory Factors in Overweight and Obese Women: A Cross-Sectional Study." *BMC Women's Health* 22, no. 1: Article 1. https://doi.org/10.1186/s12905-022-01894-9.

Morris, G., M. Berk, A. F. Carvalho, M. Maes, A. J. Walker, and B. K. Puri. 2018. "Why Should Neuroscientists Worry About Iron? The Emerging Role of Ferroptosis in the Pathophysiology of Neuroprogressive Diseases." *Behavioural Brain Research* 341: 154–175. https://doi.org/10.1016/j.bbr.2017.12.036.

Navarro-Hortal, M. D., J. M. Romero-Márquez, A. Esteban-Muñoz, et al. 2022. "Strawberry (Fragaria × Ananassa cv. Romina) Methanolic Extract Attenuates Alzheimer's Beta Amyloid Production and Oxidative Stress by SKN-1/NRF and DAF-16/FOXO Mediated Mechanisms in *C. elegans*." *Food Chemistry* 372: 131272. https://doi.org/10.1016/j.foodchem.2021.131272.

Navarro-Hortal, M. D., J. M. Romero-Márquez, M. A. López-Bascón, et al. 2024. "In Vitro and In Vivo Insights Into a Broccoli Byproduct as a Healthy Ingredient for the Management of Alzheimer's Disease and Aging Through Redox Biology." *Journal of Agricultural and Food Chemistry* 72, no. 10: 5197–5211. https://doi.org/10.1021/acs.jafc.3c05609.

Navarro-Hortal, M. D., J. M. Romero-Márquez, P. Muñoz-Ollero, et al. 2022. "Amyloid β-But Not Tau-Induced Neurotoxicity Is Suppressed by Manuka Honey via HSP-16.2 and SKN-1/Nrf2 Pathways in an In Vivo Model of Alzheimer's Disease." *Food & Function* 13, no. 21: 11185–11199. https://doi.org/10.1039/d2fo01739c.

Nunomura, A., R. J. Castellani, X. Zhu, P. I. Moreira, G. Perry, and M. A. Smith. 2006. "Involvement of Oxidative Stress in Alzheimer Disease." *Journal of Neuropathology & Experimental Neurology* 65, no. 7: 631–641. https://doi.org/10.1097/01.jnen.0000228136.58062.bf.

Oliveras-López, M.-J., J. J. M. Molina, M. V. Mir, E. F. Rey, F. Martín, and H. L.-G. de la Serrana. 2013. "Extra Virgin Olive Oil (EVOO) Consumption and Antioxidant Status in Healthy Institutionalized Elderly Humans." *Archives of Gerontology and Geriatrics* 57, no. 2: 234–242. https://doi.org/10.1016/j.archger.2013.04.002.

Onukwufor, J. O., R. T. Dirksen, and A. P. Wojtovich. 2022. "Iron Dysregulation in Mitochondrial Dysfunction and Alzheimer's Disease." *Antioxidants* 11, no. 4: 692. https://doi.org/10.3390/antiox11040692.

Parker, W. D., N. J. Mahr, C. M. Filley, et al. 1994. "Reduced Platelet Cytochrome c Oxidase Activity in Alzheimer's Disease." *Neurology* 44, no. 6: 1086–1090. https://doi.org/10.1212/wnl.44.6.1086.

Pasinetti, G. M., and P. S. Aisen. 1998. "Cyclooxygenase-2 Expression Is Increased in Frontal Cortex of Alzheimer's Disease Brain." *Neuroscience* 87, no. 2: 319–324. https://doi.org/10.1016/s0306-4522(98)00218-8.

Perez-Herrera, A., O. A. Rangel-Zuñiga, J. Delgado-Lista, et al. 2013. "The Antioxidants in Oils Heated at Frying Temperature, Whether Natural or Added, Could Protect Against Postprandial Oxidative Stress in Obese People." *Food Chemistry* 138, no. 4: 2250–2259. https://doi.org/10.1016/j.foodchem.2012.12.023.

Picone, P., D. Nuzzo, L. Caruana, V. Scafidi, and M. Di Carlo. 2014. "Mitochondrial Dysfunction: Different Routes to Alzheimer's Disease Therapy." *Oxidative Medicine and Cellular Longevity* 2014: e780179. https://doi.org/10.1155/2014/780179.

Porta-de-la-Riva, M., L. Fontrodona, A. Villanueva, and J. Cerón. 2012. "Basic *Caenorhabditis elegans* Methods: Synchronization and Observation." *Journal of Visualized Experiments: JoVE* 64: 4019. https://doi.org/10.3791/4019.

Qi, Z., B. Yang, F. Giampieri, et al. 2024. "The Preventive and Inhibitory Effects of Red Raspberries on Cancer." *Journal of Berry Research* 14, no. 1: 61–71. https://doi.org/10.3233/JBR-240004.

Regolo, L., F. Giampieri, M. Battino, et al. 2024. "From By-Products to New Application Opportunities: The Enhancement of the Leaves Deriving From the Fruit Plants for New Potential Healthy Products." *Frontiers in Nutrition* 11: 1083759. https://doi.org/10.3389/fnut.2024.1083759.

Rietjens, S. J., A. Bast, and G. R. M. M. Haenen. 2007. "New Insights Into Controversies on the Antioxidant Potential of the Olive Oil Antioxidant Hydroxytyrosol." *Journal of Agricultural and Food Chemistry* 55, no. 18: 7609–7614. https://doi.org/10.1021/jf0706934.

Rigacci, S., V. Guidotti, M. Bucciantini, et al. 2011. "Aβ(1–42) Aggregates Into Non-Toxic Amyloid Assemblies in the Presence of the Natural Polyphenol Oleuropein Aglycon." *Current Alzheimer Research* 8, no. 8: 841–852.

Rivas-García, L., J. M. Romero-Márquez, M. D. Navarro-Hortal, et al. 2022. "Unravelling Potential Biomedical Applications of the Edible Flower *Tulbaghia violacea*." *Food Chemistry* 381: 132096. https://doi.org/10.1016/j.foodchem.2022.132096.

Romero-Márquez, J. M., T. Y. Forbes-Hernández, M. D. Navarro-Hortal, et al. 2023a. "Molecular Mechanisms of the Protective Effects of Olive Leaf Polyphenols Against Alzheimer's Disease." *International Journal of Molecular Sciences* 24, no. 5: 4353. https://doi.org/10.3390/ijms24054353.

Romero-Márquez, J. M., M. D. Navarro-Hortal, T. Y. Forbes-Hernández, et al. 2023b. "Exploring the Antioxidant, Neuroprotective, and Anti-Inflammatory Potential of Olive Leaf Extracts From Spain, Portugal, Greece, and Italy." *Antioxidants* 12, no. 8: Article 8. https://doi.org/10.3390/antiox12081538.

Romero-Márquez, J. M., M. D. Navarro-Hortal, T. Y. Forbes-Hernández, et al. 2024. "Effect of Olive Leaf Phytochemicals on the Anti-Acetylcholinesterase, Anti-Cyclooxygenase-2 and Ferric Reducing Antioxidant Capacity." *Food Chemistry* 444: 138516. https://doi.org/10.1016/j.foodchem.2024.138516.

Romero-Márquez, J. M., M. D. Navarro-Hortal, V. Jiménez-Trigo, et al. 2022a. "An Oleuropein Rich-Olive (*Olea europaea* L.) Leaf Extract Reduces β-Amyloid and Tau Proteotoxicity Through Regulation of Oxidative- and Heat Shock-Stress Responses in *Caenorhabditis elegans*." *Food and Chemical Toxicology: An International Journal Published for the British Industrial Biological Research Association* 162: 112914. https://doi.org/10.1016/j.fct.2022.112914.

Romero-Márquez, J. M., M. D. Navarro-Hortal, V. Jiménez-Trigo, et al. 2022b. "An Olive-Derived Extract 20% Rich in Hydroxytyrosol Prevents β-Amyloid Aggregation and Oxidative Stress, Two Features of Alzheimer Disease, via SKN-1/NRF2 and HSP-16.2 in *Caenorhabditis elegans*." *Antioxidants (Basel, Switzerland)* 11, no. 4: Article 4. https://doi.org/10.3390/antiox11040629.

Romero-Márquez, J. M., A. Varela-López, M. D. Navarro-Hortal, et al. 2021. "Molecular Interactions Between Dietary Lipids and Bone Tissue During Aging." *International Journal of Molecular Sciences* 22, no. 12: 6473. https://doi.org/10.3390/ijms22126473.

Rosi, A., F. Scazzina, F. Giampieri, et al. 2024. "Adherence to the Mediterranean Diet in 5 Mediterranean Countries: A Descriptive Analysis of the DELICIOUS Project." *Mediterranean Journal of Nutrition and Metabolism* 17, no. 4: 323–334. https://doi.org/10.1177/1973798x241296440.

Saz-Lara, A., M. Battino, A. Lara, et al. 2024. "Differences in Carotid to Femoral Pulse Wave Velocity and Carotid Intima Media Thickness Between Vegetarian and Omnivorous Diets in Healthy Subjects: A Systematic Review and Meta-Analysis." *Food & Function* 15, no. 3: 1135–1143. https://doi.org/10.1039/D3FO05061K.

Scoditti, E., A. Nestola, M. Massaro, et al. 2014. "Hydroxytyrosol Suppresses MMP-9 and COX-2 Activity and Expression in Activated Human Monocytes via PKCα and PKCβ1 Inhibition." *Atherosclerosis* 232, no. 1: 17–24. https://doi.org/10.1016/j.atherosclerosis.2013.10.017.

Smith, M. A., P. L. R. Harris, L. M. Sayre, and G. Perry. 1997. "Iron Accumulation in Alzheimer Disease Is a Source of Redox-Generated Free Radicals." *Proceedings of the National Academy of Sciences of the United States of America* 94, no. 18: 9866–9868.

Steinman, M. A., K. R. McQuaid, and K. E. Covinsky. 2006. "Age and Rising Rates of Cyclooxygenase-2 Inhibitor Use." *Journal of General Internal Medicine* 21, no. 3: 245–250. https://doi.org/10.1111/j.1525-1497.2006.00336.x.

Stewart, W. F., C. Kawas, M. Corrada, and E. J. Metter. 1997. "Risk of Alzheimer's Disease and Duration of NSAID Use." *Neurology* 48, no. 3: 626–632. https://doi.org/10.1212/wnl.48.3.626.

Strayer, A., Z. Wu, Y. Christen, C. D. Link, and Y. Luo. 2003. "Expression of the Small Heat-Shock Protein Hsp16-2 in *Caenorhabditis elegans* Is Suppressed by Ginkgo Biloba Extract EGb 761." *FASEB Journal: Official Publication of the Federation of American Societies for Experimental Biology* 17, no. 15: 2305–2307. https://doi.org/10.1096/fj.03-0376fje.

Terry, A. V., and J. J. Buccafusco. 2003. "The Cholinergic Hypothesis of Age and Alzheimer's Disease-Related Cognitive Deficits: Recent Challenges and Their Implications for Novel Drug Development." *Journal of Pharmacology and Experimental Therapeutics* 306, no. 3: 821–827. https://doi.org/10.1124/jpet.102.041616.

Tullet, J. M. A., J. W. Green, C. Au, et al. 2017. "The SKN-1/Nrf2 Transcription Factor Can Protect Against Oxidative Stress and Increase Lifespan in *C. elegans* by Distinct Mechanisms." *Aging Cell* 16, no. 5: 1191–1194. https://doi.org/10.1111/acel.12627.

Umeno, A., M. Takashima, K. Murotomi, et al. 2015. "Radical-Scavenging Activity and Antioxidative Effects of Olive Leaf Components Oleuropein and Hydroxytyrosol in Comparison With Homovanillic Alcohol." *Journal of Oleo Science* 64, no. 7: 793–800. https://doi.org/10.5650/jos.ess15042.

Van Raamsdonk, J. M., and S. Hekimi. 2009. "Deletion of the Mitochondrial Superoxide Dismutase Sod-2 Extends Lifespan in *Caenorhabditis elegans*." *PLoS Genetics* 5, no. 2: e1000361. https://doi.org/10.1371/journal.pgen.1000361.

Vassilaki, M., J. A. Aakre, J. A. Syrjanen, et al. 2018. "Mediterranean Diet, Its Components and Amyloid Imaging Biomarkers." *Journal of Alzheimer's Disease: JAD* 64, no. 1: 281–290. https://doi.org/10.3233/JAD-171121.

Von Montfort, C., N. Matias, A. Fernandez, et al. 2012. "Mitochondrial GSH Determines the Toxic or Therapeutic Potential of Superoxide Scavenging in Steatohepatitis." *Journal of Hepatology* 57, no. 4: 852–859. https://doi.org/10.1016/j.jhep.2012.05.024.

Xiang, Z., L. Ho, S. Yemul, et al. 2018. "Cyclooxygenase-2 Promotes Amyloid Plaque Deposition in a Mouse Model of Alzheimer's Disease Neuropathology." *Gene Expression* 10, no. 5–6: 271–278.

Yonezawa, Y., T. Kihara, K. Ibi, et al. 2019. "Olive-Derived Hydroxytyrosol Shows Anti-Inflammatory Effect Without Gastric Damage in Rats." *Biological & Pharmaceutical Bulletin* 42, no. 7: 1120–1127. https://doi.org/10.1248/bpb.b18-00979.

Youssef, P., B. Chami, J. Lim, T. Middleton, G. T. Sutherland, and P. K. Witting. 2018. "Evidence Supporting Oxidative Stress in a Moderately Affected Area of the Brain in Alzheimer's Disease." *Scientific Reports* 8, no. 1: Article 1. https://doi.org/10.1038/s41598-018-29770-3.

Zhang, X., J. Cao, and L. Zhong. 2009. "Hydroxytyrosol Inhibits Pro-Inflammatory Cytokines, iNOS, and COX-2 Expression in Human Monocytic Cells." *Naunyn-Schmiedeberg's Archives of Pharmacology* 379, no. 6: 581–586. https://doi.org/10.1007/s00210-009-0399-7.

Zhao, Z. 2019. "Iron and Oxidizing Species in Oxidative Stress and Alzheimer's Disease." *Aging Medicine* 2, no. 2: 82–87. https://doi.org/10.1002/agm2.12074.

Supporting Information

Additional supporting information can be found online in the Supporting Information section.